Interplay between serine/threonine protein kinases and two-component systems in *Mycobacterium tuberculosis* environmental response

A thesis submitted by

Natalie Sontag

in partial fulfillment of the requirements for the degree of

Doctor of Philosophy

in

Molecular Microbiology

Tufts University

Graduate School of Biomedical Sciences

March 2026

Advisor: Shumin Tan, Ph.D.

Abstract

Mycobacterium tuberculosis (Mtb), the causative agent of tuberculosis (TB), remains a leading cause of death from infectious disease worldwide. A defining feature of Mtb pathogenesis is its capacity to survive within diverse and dynamic host microenvironments, where the bacterium encounters fluctuating stresses including nitric oxide (NO), hypoxia, acidic pH, and changes in chloride (Cl^-) and potassium (K^+) levels. Successful adaptation to these conditions requires precise signal transduction regulatory systems that translate environmental cues into coordinated transcriptional and physiological responses. While two-component systems (TCSs) are well-established mediators of bacterial environmental sensing, Mtb also encodes an expanded repertoire of eukaryotic-like serine/threonine protein kinases (STPKs) compared to other bacterial pathogens. In addition, global phosphoproteomic studies in Mtb identify TCSs as substrates of STPK phosphorylation, raising the possibility that these systems function in an integrated manner. We thus sought to understand if, and how, STPK signaling intersects with canonical TCS regulation to shape Mtb environmental adaptation.

This thesis examines how STPKs influence the activity of TCS response regulators (RRs) in Mtb. Using mycobacterial protein fragment complementation (M-PFC) interaction mapping, we identified physical associations between multiple STPKs and the Mtb RRs PrrA, DosR, PhoP, and KdpE, revealing both overlap and selectivity in STPK-RR interaction profiles. Focusing on DosR, we uncovered that upon *in vitro* phosphorylation by the STPKs PknH and PknD, DNA binding and steady-state transcription of DosR-regulated genes was altered. Consistent with a role of STPKs in modulating DosR activity, deletion of the STPK *pknH* altered DosR-dependent transcription under NO exposure and led to increased induction of DosR-regulated genes

at intermediate signal levels, supporting that PknH modulates the magnitude and sensitivity of the DosR response.

Taken together, this thesis reveals a model in which STPK-TCS crosstalk enables graded and context-dependent regulation of gene expression, providing Mtb with regulatory flexibility essential for survival in the heterogeneous host environment during infection. More broadly, these studies highlight post-translational control as a key layer of regulation in Mtb environmental response and suggest that disruption of signaling integration may represent an underexplored vulnerability in this pathogen. Future studies aimed at disentangling structural and regulatory effects of phosphorylation on RR function will further refine our understanding of how Mtb coordinates adaptive responses during infection.

This work is dedicated to my family without whom it would not have been possible.

Acknowledgements

The entirety of this thesis process would not have been possible without the combined efforts, guidance, and support of many people. I would like to take the time to thank those who have been such an integral part of this journey with me, especially as I know many will be there on the journey to come.

First, I would like to thank my advisor Shumin Tan. In many ways she has seen me grow up in science as I joined the lab shortly after my undergraduate studies. She has been a thoughtful mentor to me, guiding me through what it means to be an independent scientist, and what it means to be a responsible one. For those lessons, I am eternally grateful.

I am also thankful to my committee members Ralph Isberg, Carol Kumamoto, and Andrew Camilli for their contributions to this work. Each of their input was invaluable, and it was a privilege to spend time with them discussing what culminated into this thesis. Learning from them and being encouraged by them has greatly shaped the trajectory of my scientific career.

My graduate school experience would not have been whole without each of the Tan lab members, past and present. I would like to acknowledge Natalie Quirk, Liz Billings, Rachel Yue Chen, Anna-Lisa Lawrence, Anna Kim, Alwyn Ecker, Yuzo Kevorkian, and Richard Lavin. I am especially grateful to Alwyn Ecker whose efforts kickstarted the early work of this thesis. The combined support and energy of this lab truly helped me to thrive, and I look forward to maintaining those relationships in the years to come.

I would like to thank the Tufts Microbiology department and the wonderful community fostered there. This community has brought me friendship, encouragement, and professional development. I couldn't have asked for more. I would like to specifically thank Verna Manni and Jackie Kulas for their tireless efforts to ensure the department functions productively and smoothly.

My friendships outside of Tufts have been such a huge source of relief from the stressors of graduate school. My best friends Kate Wood and Natalie Vaughan have seen it all. Wherever we are in the world, I feel their love and support.

Finally, I would like to thank my family and my partner Nicholas DiBenedetto. Without their unconditional love, understanding, and support, I can truly say I would not be where I am today.

Table of Contents

Title Page i

Abstract ii

Dedication iii

Acknowledgements v

Table of Contents vii

List of Figures x

List of Copyright Materials Used xi

List of Abbreviations xii

Chapter 1: Introduction 1

1.1 Introduction to *Mycobacterium tuberculosis* and consequences of host infection 2

1.1.1 Tuberculosis overview and its role globally past and present 2

1.1.2 The infectious life cycle of Mtb 4

1.1.3 Host response to Mtb infection 6

1.2 Mtb environmental signal response and regulation 8

1.2.1 Nitric oxide (NO) 9

1.2.2 Hypoxia 11

1.2.3 Protons/acidic pH (H^+) 13

1.2.4 Chloride (Cl^-) 15

1.2.5 Potassium (K^+) 16

1.3 Bacterial environmental sensing through signal transduction regulatory mechanisms 17

1.3.1 Two-component systems (TCSs) and transcriptional regulation in response to environmental signals 17

1.3.2 Serine/threonine protein kinases (STPKs) and post-translational modification in response to environmental signals 22

1.4 Integration of TCSs and STPKs 25

1.4.1 Interplay between TCSs and STPKs across bacterial species 25
1.4.2 Evidence of TCS-STPK interplay in Mtb 26
1.5 Thesis overview.....27

Chapter 2: Serine/threonine protein kinase phosphorylation of DosR alters target gene transcription mechanics and regulates *Mycobacterium tuberculosis* response to nitric oxide stress 29
2.1 Introduction 30
2.2 Results 33
2.2.1 There is both overlap and specificity in interactions between STPKs and TCS RRs 33
2.2.2 Changes in DosR phosphorylation status alter its binding affinity to target promoters 35
2.2.3 STPK phosphorylation of purified DosR decreases the level and alters concentration-dependence of steady-state transcription rates of its target genes 38
2.2.4 The STPK PknH regulates the DosR-dependent transcriptional responses of Mtb to NO.....41
2.3 Discussion 44
2.4 Materials and Methods 49
2.4.1 Mycobacterial protein fragment complementation assays 49
2.4.2 Recombinant protein expression and purification 49
2.4.3 Mass spectrometry.....51
2.4.4 Electrophoretic mobility shift assays.....52
2.4.5 Fluorescence polarization assays.....52
2.4.6 RNA aptamer-based transcriptional assay.....54
2.4.7 Mtb strains and culture 55
2.4.8 qRT-PCR analyses.....56
2.4.9 *hspX'*::GFP reporter assay 56
2.4.10 Statistical analyses.....56
2.5 Attribution of work.....57

Chapter 3: Discussion 58
3.1 Introduction 59
3.2 Importance of STPK phosphorylation site on TCS RR structure and function 60
3.3 Regulation of STPK activity 66
3.4 Role of STPK-mediated regulation throughout host infection.....68

3.5 Conclusion....71

Chapter 4: Appendix....72
4.1 Chapter 2 Supplemental Information....73
4.1.1 Chapter 2 Supplemental Figures....73
4.1.2 Chapter 2 Supplemental Files List....78

Chapter 5: Bibliography....79

List of Figures

Figure 2.1 Specificity of interactions between TCS RRs and STPKs. 33

Figure 2.2 Changes in DosR phosphorylation status alter binding to the promoter of its target gene *hspX*. 36

Figure 2.3 Fluorescence polarization assays demonstrate inhibition of DosR binding to its target gene promoters upon PknH or PknD phosphorylation. 38

Figure 2.4 STPK phosphorylation of purified DosR decreases the level and alters concentration-dependence of steady-state transcription rates of its targets genes. 40

Figure 2.5 The STPK PknH regulates response of the *hspX'*::GFP reporter to NO. 41

Figure 2.6 The STPK PknH regulates the DosR-dependent transcriptional response of Mtb to NO. 42

Figure 3.1 Phosphorylated residues of interest on DosR. 62

Figure 3.2 Preservation of STPK phosphorylation sites on TCS RRs is critical for transcriptional response to environmental signals. 63

Figure 3.3 Preservation of STPK phosphorylation sites on TCS RRs is important for Mtb growth control in response to environmental signals. 64

Figure 4.1 There is both overlap and specificity in interactions between STPKs and TCS RRs. 73

Figure 4.2 Annotated MS/MS spectrum confirming phosphorylation of DosR T198 after PknH treatment. 73

Figure 4.3 Annotated MS/MS spectrum confirming phosphorylation of DosR T205 after PknH treatment. 74

Figure 4.4 Annotated MS/MS spectrum confirming phosphorylation of DosR T198 and T205 after PknH treatment. 75

Figure 4.5 Annotated MS/MS spectrum confirming phosphorylation of DosR D54 after PknH and acetyl phosphate treatment. 75

Figure 4.6 Changes in DosR phosphorylation status alter DNA binding affinity to the promoter of its target gene *fdxA*. 76

Figure 4.7 DosR binding to the *hspX* and *fdxA* promoters is specific. 77

Figure 4.8 Mutation of DosR T198/T205 sites render the protein non-functional. 78

List of Copyright Materials Used

Sontag NR, Ruiz Manzano A, Ecker AMV, Galburt EA, Tan S. (2026) Serine/threonine protein kinase phosphorylation of DosR alters target gene transcription mechanics and regulates *Mycobacterium tuberculosis* response to nitric oxide stress. PLoS Genetics 22(2): e1012043. doi: 10.1371/journal.pgen.1012043.

List of Abbreviations

AcP	Acetyl phosphate
ChIP	Chromatin immunoprecipitation
Cl^-	Chloride
FP	Fluorescence polarization
H^+	Protons
H^+-ATPase	Vacuolar-ATPase
HK	Histidine kinase
HIV	Human immunodeficiency virus
IFN-γ	Interferon gamma
iNOS	Inducible nitric oxide synthase
K^+	Potassium
MDHFR	Murine dihydrofolate reductase
M-PFC	Mycobacterial protein fragment complementation assay
MS	Mass spectrometry
Mtb	*Mycobacterium tuberculosis*
NO	Nitric oxide
RR	Response regulator
STPK	Serine/threonine protein kinase
TB	Tuberculosis
TCS	Two-component system
TNF	Tumor necrosis factor
TRIM	Trimethoprim
WT	Wild type

Chapter 1: Introduction

1.1: Introduction to *Mycobacterium tuberculosis* and consequences of host infection

1.1.1: Tuberculosis overview and its role globally past and present

Tuberculosis (TB) is a communicable disease that is caused by the bacterium *Mycobacterium tuberculosis* (Mtb) and represents one of the most enduring infectious threats to human health. While molecular evidence indicates its survival amongst human populations for at least 9,000 years, further analysis of the Mtb genome suggests that the Mtb complex likely emerged much earlier, potentially up to 40,000 years ago [1, 2]. TB, despite its existence as an ancient disease, continued to cause a significant decline in human populations in both Europe and North America in the late 19th and early 20th centuries, with as much as 25% of the population affected [3, 4]. At that time, TB was often referred to as "consumption" due to the significant wasting of the human body [5]. The earliest efforts to treat TB relied largely on environmental interventions, most notably the establishment of open-air sanitoria in the mid-1800s [5]. While these institutions did improve upon general patient care, they provided relatively little direct benefit in alleviating the underlying TB infection.

However, a transformative shift in the management of TB infection occurred in the mid-20th century with the emergence of antibiotic treatment. For example, the significant discovery of streptomycin in 1944 marked the first successful pharmacological treatment of TB, with demonstrated efficacy in laboratory studies, animal models, and human patients [6]. After the establishment of streptomycin as an efficacious treatment to address TB infection, further efforts to develop additional antitubercular approaches using combination drug regimens administered over extended periods became central to contemporary treatment approaches [7].

Mtb is primarily transmitted by airborne particles that are expelled when an individual with active disease coughs, thereby allowing the bacterium to be inhaled by and establish infection in the lungs of another individual [8, 9]. Pulmonary TB is the most common clinical presentation of the disease [8]. However, Mtb can spread beyond the respiratory tract to give rise to extrapulmonary disease involving tissues such as lymph nodes and the central nervous system [8, 10]. Following exposure to Mtb, most infected individuals do not immediately develop symptoms, but rather harbor the bacterium in what is classified as a clinically "latent" state [11]. While latent infection can persist for decades without apparent disease progression, approximately 5-10% of those infected individuals will ultimately progress to active TB, with a significant proportion developing disease within the first two years after infection [11, 12].

Despite the availability of effective antibiotics and diagnostic tools, TB continues to impose a heavy global health burden. Each year, roughly 10 million people develop active TB disease, leading to approximately 1.5 million deaths worldwide [13]. The impact of the burden imposed by TB is most severely felt in regions in which healthcare infrastructure is poor, where barriers to diagnosis persist, and where treatment adherence is particularly difficult [14]. Together with these challenges, the absence of a broadly protective vaccine, as well as the increasing prevalence of multi-drug resistant Mtb strains, make eradicating TB even more difficult [15]. Recently, disruptions caused by the COVID-19 pandemic led to declines in TB diagnosis and treatment, reversing years of incremental progress in global TB control [16]. TB also remains a concern in high-income countries, particularly in those individuals with compromised immune systems,

including those living with Human Immunodeficiency Virus (HIV) who face an increased risk of severe and disseminated disease [17, 18].

Although significant progress has been made in understanding and treating TB, complete eradication of the pathogen has remained out of reach. This is due in part to the fact that the relative contributions of bacterial adaptation, host immune response, and environmental factors remain incompletely understood. Addressing these gaps is essential for advancing therapeutic strategies and developing interventions capable of more effectively preventing/stopping disease progression and transmission.

1.1.2: The infectious life cycle of Mtb

At the beginning of its infectious life cycle, Mtb is first transmitted via aerosolized droplets that are produced when an individual with active pulmonary TB coughs, speaks, or sneezes [8, 9]. Once the bacilli are inhaled, Mtb reaches the lung alveoli where it then encounters the first line of host defense known as alveolar macrophages [19]. As resident phagocytes, the purpose of these alveolar macrophages is to engulf Mtb and to prevent its dissemination to other sites in the host [19, 20]. Immediately after internalizing the bacterium, the early phagosome begins a maturation program that ideally culminates in fusion with host lysosomes, subsequently resulting in bacterial degradation; however, Mtb actively disrupts this process at an early stage [21-23].

While Mtb-containing phagosomes retain some characteristics of early endosomes, the bacterium has developed numerous mechanisms to prevent their further development [24-26]. For example, through the modulation of host signaling pathways

the bacterium restricts recruitment of late endosomal markers such as Rab7, resulting in inhibition of phagosome-lysosomal maturation [25, 26]. Another characteristic of the maturing phagosome, namely compartment acidification, is also impeded by Mtb [22, 23]. In a typical bacterial infection, the vacuolar H^+-ATPase (V-ATPase) progressively lowers the luminal pH of maturing phagosomes, reaching pH values below 5 in fully matured phagolysosomes [21, 27]. This highly acidic environment is required for the activity of many lysosomal proteins, such as hydrolases and lipases, which function to degrade internalized pathogens like Mtb [21, 27]. Importantly, phagosomal acidification is also critical for the activation of lysosomal cathepsins, a family of proteases that require acidic pH for proteolytic maturation and activity [28-30]. Active cathepsins contribute substantially to antimicrobial defense by degrading engulfed pathogens and processing microbial components for antigen presentation [29, 31]. The acidification process also permits the release of iron and other nutrients from host proteins and contributes to directed host-mediated antimicrobial activity through pH stress [32, 33]. By utilizing various tools in its repertoire, Mtb can successfully prevent the full acidification of the phagosomal lumen.

As the infection progresses, Mtb-containing phagosomes evolve into housing compartments that can support bacterial persistence. While residing within these phagosomes, Mtb will encounter fluctuating stresses, including nutrient limitation, as well as exposure to immune effector molecules [34-38]. In response, the bacterium undergoes extensive transcriptional and metabolic reprogramming, shifting toward a non-replicating or slowly replicating state [34, 39, 40]. Extensive regulatory networks involving two-component systems (TCSs), alternative sigma factors, and stress response

regulons enable Mtb to maintain viability whilst minimizing metabolic activity [41, 42]. This adaptive state underlies the bacterium's capacity for long-term intracellular survival and also contributes heavily to antibiotic tolerance [43]. Although traditionally considered an intra-phagosomal pathogen, Mtb can disrupt the phagosomal membrane and access the host cytosol, particularly during later stages of infection [44, 45]. Mediated in part by the ESX-1 secretion system, this process is associated with host cell damage, immune activation, and bacterial dissemination [44, 45]. Access to the host cytosol may promote spread to neighboring cells and thereby influence the balance between containment by the host and disease progression. Additionally, Mtb infection is not exclusively intracellular. As disease progresses, a subpopulation of Mtb also resides extracellularly within the caseous necrotic core of hallmark granulomas [46]. These extracellular populations experience a distinct milieu that is thought to further shape bacterial physiology and contribute to persistence and transmission.

1.1.3: Host response to Mtb infection

The outcome of Mtb infection is determined by complex, dynamic interactions between the pathogen and the host immune system. Rather than eliminating the bacterium outright, the host response typically results in a constraining of bacterial growth with long-term persistence [47]. This balance between host immune-mediated control and pathogen survival underlies both latent Mtb infection as well as the potential for disease activation, ultimately making TB a perfect example of chronic infection that is shaped by imperfect immunity [11, 12].

Following initial colonization, the host mounts a coordinated immune response that includes the development of immune cells at the site of infection such as epithelioid macrophages and multinucleated giant cells, while other cell types such as lymphocytes are also recruited to the lung [48, 49]. Upon the coordinated development and recruitment of these immune cells, a hallmark of TB infection is the subsequent formation of a granuloma [46, 50, 51]. A granuloma is a highly structured immune microenvironment, where the host attempts to contain Mtb and consequently limit tissue damage by creating an environment in which the immune pressure limits bacterial growth [46, 50, 51]. Within the granuloma, immune cells and Mtb engage in a prolonged standoff, characterized by fluctuating inflammatory signals and metabolic stress.

While host-induced inflammation is necessary for TB control, excessive or dysregulated immune responses contribute to tissue damage and disease pathology [52]. Specifically, necrosis of infected immune cells such as macrophages and neutrophils, driven by inflammatory cytokines and host cell death pathways can lead to caseation and cavitation in pulmonary tissue, ultimately facilitating bacterial transmission [49, 52-55]. Regulatory immune mechanisms, including the activity of regulatory T-cells and anti-inflammatory cytokines such as IL-10, modulate inflammation with the aim of limiting tissue damage, but may also impair bacterial clearance [56]. Thus, disease severity reflects a balance between protective immunity and immunopathology.

The infectious cycle described here reflects the classical mechanism of infection, and a large proportion of TB patients continue as latently infected patients [11], while a proportion of those patients with TB fail to contain the infection or experience immune perturbations, such as those co-infected with HIV or those undergoing

immunosuppressive therapy, which allow latent bacilli to resume replication [17, 18]. Critically, regardless of existing in either an active or latent state, Mtb successfully adapts to the local host environment through appropriate sensing of environmental signals throughout the course of infection.

1.2: Mtb environmental signal response and regulation

Through its infectious life cycle, the survival and persistence of Mtb within the human host is dependent on its ability to sense and adapt to a dynamic local environment. Upon phagocytosis, Mtb is exposed to immune-mediated stresses such as hypoxia, reactive nitrogen species, as well as nutrient limitation, but also to rapid and spatially heterogeneous changes in ionic conditions generated by host defense mechanisms [57-59]. Fluctuations in concentrations of nitric oxide (NO), protons (H^+), chloride (Cl^-), and potassium (K^+) within the phagosome serve as both antimicrobial pressures and informational cues that reflect the maturation state of the phagosome and the degree of immune activation by the host [57-60]. As previously mentioned, Mtb infection is not solely intracellular as Mtb can also reside extracellularly within the caseous necrotic core of hallmark granulomas [46]. These extracellular niches differ markedly from the phagosomal environment and are characterized by limited vascularization and reduced oxygen tension [61, 62]. Hypoxia is thought to be especially relevant in these necrotic granuloma cores, where diffusion barriers and local inflammation create low-oxygen microenvironments [62]. Thus, the spectrum of stressors encountered by Mtb is strongly shaped by its physical location within the host.

Understanding how Mtb integrates diverse, host-derived signals into regulatory networks is critical, as these pathways sit at the interface between host antimicrobial strategies and bacterial adaptation, and represent potential vulnerabilities that could be exploited for future therapeutic intervention. In this section, I will expand on host-derived signals present in microenvironments encountered by Mtb of particular pertinence for my thesis work, namely NO, hypoxia, acidic pH (H^+), Cl^-, and K^+.

1.2.1: Nitric oxide (NO)

Throughout the course of infection, Mtb resides within a variety of host immune cells where it encounters a range of host immune-generated stresses that fluctuate in their magnitude as well as their duration. Nitric oxide (NO) is a host immune signal frequently encountered by Mtb that shapes its physiology [63]. In the context of infection, NO signaling is antimicrobial, but its presence also broadly serves as a reliable indicator of host immune activation [64]. Over time, Mtb has evolved dedicated sensory and regulatory systems that detect NO and initiate transcriptional and metabolic adaptations that promote bacterial survival under this stress [65, 66].

Once infected by Mtb, macrophages are activated by pro-inflammatory cytokines, particularly interferon-gamma (IFN-γ) and tumor necrosis factor (TNF), which induce the expression of inducible nitric oxide synthase (iNOS) [67, 68]. iNOS acts to catalyze the conversion of L-arginine to NO, resulting in sustained NO production within both the phagosomal and cytosolic compartments [69]. In murine models, it has been shown that NO is essential for control of Mtb replication, as iNOS-deficient mice exhibit poorer control of bacterial growth and die significantly more rapid than WT mice following

infection [70]. Notably, NO contributes to antimicrobial activity both directly and indirectly, reacting with superoxide to generate highly reactive species such as peroxynitrite that exacerbate cellular damage to invading pathogens [71, 72].

The principal mechanism by which Mtb "sees" NO is through the DosRS(T) TCS where the histidine kinases (HKs) DosS and DosT sense and respond to NO and hypoxia respectively [65, 66]. The DosR response regulator (RR) functions as a transcription factor, and upon its activation, induces a defined regulon comprising 48 genes associated with metabolic remodeling, redox homeostasis and stress resistance [39, 73]. Specifically, many DosR-regulated genes encode proteins involved in anaerobic metabolism, lipid utilization, and alternative respiratory pathways [63, 66, 74]. For example, *hspX* encodes the α-crystallin-like chaperone HspX that stabilizes proteins and is strongly associated with bacterial growth arrest and persistence under hypoxic or nitrosative stress [75, 76]. The ferrodoxin encoded by *fdxA* participates in redox reactions that aid in the maintenance of intracellular electron balance when components of the aerobic respiratory chain become inhibited [77, 78]. Additional genes within the regulon encode enzymes involved in lipid metabolism and intermediary metabolism, including Tgs1, which catalyzes triacylglycerol synthesis and contributes to the accumulation of intracellular lipid stores in support of long-term survival throughout non-replicating states [79, 80].

As mentioned above, DosR-regulated loci encode proteins associated with alternative respiratory processes and redox buffering, enabling the bacterium to sustain proton motive force and maintain metabolic homeostasis when NO disrupts heme- and iron-sulfur-containing respiratory enzymes [63, 66, 74]. In this way, NO functions not only as an antimicrobial molecule but also as an environmental signal that triggers a

persistence-associated metabolic program in Mtb. The functional composition of the DosR regulon contrasts with NO responses in many enteric bacteria such as *Escherichia coli* and *Salmonella enterica*. In those organisms, exposure to NO primarily induces rapid detoxification systems that directly convert reactive nitrogen species into less toxic products. A central component of this response is the flavohemoglobin Hmp, which oxidizes NO to nitrate under aerobic conditions and reduces it to nitrous oxide under hypoxic conditions, thereby protecting respiratory enzymes from nitrosative damage [81-83]. In *E. coli*, NO detoxification is further supported by the NorVW flavorubredoxin system [84], which reduces NO under anaerobic conditions and is transcriptionally activated by the NO-sensing regulator NorR [85]. Additional protective pathways repair cellular damage caused by nitrosative stress; for example, the YtfE protein in *E. coli* and *S. enterica* participates in the repair of iron-sulfur clusters damaged by NO [86, 87]. Expression of a number of these genes is coordinated by the transcriptional regulator NsrR, which represses nitrosative stress genes under basal conditions and becomes inactivated upon exposure to NO [88, 89]. Together, these pathways enable enteric bacteria such as *E. coli* and *S. enterica* to rapidly detoxify NO while maintaining active respiration and continued replication during host infection.

1.2.2: Hypoxia

Oxygen availability is physiologically consequential for Mtb as oxygen tension in host tissues is dynamic [62]. Throughout the course of infection, the oxygen tension can decline substantially due to inflammatory cell influx or vascular disruption [90, 91]. Importantly, this low oxygen tension can be sustained in the granuloma [90, 91]. For

example, in advanced granulomas, particularly those with caseous necrotic cores, restricted diffusion barriers can generate microenvironments with reduced oxygen tension [61, 62]. In Mtb, central metabolism and energy generation are closely tied to oxidative phosphorylation. Consequently, hypoxia represents a severe metabolic constraint in the host lesion environment.

Experimental hypoxia models, such as the Wayne model of gradual oxygen depletion, demonstrate that Mtb can enter into a non-replicating persistent state under low oxygen characterized by reduced bacterial replication, altered central carbon metabolism, and increased tolerance to certain antibiotics [34]. However, when oxygen is restored, the bacterium resumes normal growth [34], highlighting that this persistent, low-replicating state is reversible.

Reduced oxygen tension frequently co-occurs with other host-derived stresses including NO exposure, nutrient limitation, and acidic or ionic stresses within inflammatory lesions. The DosRS(T) system itself exemplifies this overlap, as its sensors respond to hypoxia and NO [65], thereby linking oxygen sensing to immune activation signals. From a regulatory perspective, hypoxia operates within a broader network of environmental cues that inform the bacterium about its location within the host and the state of the surrounding immune response. This begins to illustrate a key principle in Mtb biology: environmental signals are rarely encountered in isolation. It then stands to reason that bacterial regulatory systems must be capable of integrating multiple inputs. How Mtb integrates diverse environmental signals from different signaling systems to coordinate adaptive states will be a major theme expanded upon throughout this thesis work.

1.2.3: Acidic pH/protons (H^+)

Changes in pH (H^+ concentration) play a central role in shaping Mtb physiology throughout the course of host infection. From the beginning of phagocytic uptake by alveolar macrophages, Mtb experiences a transition from the extracellular environment of the lung to a progressively acidifying intracellular compartment. This shift in pH provides an early, yet persistent signal that informs Mtb of host cell entry; because of this, Mtb actively modulates the phagosomal environment to maintain a niche permissive for survival. As discussed above, the bacterium does this by interfering with the recruitment of V-ATPase, a key driver of phagosomal acidification through the secreted effector PtpA [22, 27, 92]. PtpA dephosphorylates the host protein VPS33B, preventing phagolysosome fusion, directly binding to the H-subunit of V-ATPase and inhibiting its trafficking [22, 23]. Additionally, Mtb secretes 1-tuberculosinyladenosine, a terpene nucleoside that further neutralizes the compartment [93]. Together, these mechanisms stabilize phagosomal pH at approximately 6.2-6.4, creating a mildly acidic environment that supports bacterial survival [22]. Of note, acidification triggers slowed Mtb growth and can even lead to growth arrest [94]. In contrast, non-Mtb complex mycobacteria such as *M. smegmatis* and *M. marinum* continue to replicate efficiently at acidic pH, highlighting slowed growth as an adaptive physiological response of Mtb and other members of the Mtb complex [95, 96].

A key determinant of the ability of Mtb to tolerate acid is its cell envelope that serves as a physical barrier to changes in proton concentration. The cell envelope consists of a covalently linked peptidoglycan-arabinogalactan-mycolic acid core overlaid with extractable lipids [97]. This lipid-rich structure is highly ordered and exhibits extremely

low ion permeability, substantially restricting passive proton diffusion across the cytoplasmic membrane [98, 99]. As a result, changes in surrounding phagosomal pH are transmitted slowly and incompletely to the bacterial cytosol, providing a foundational layer of protection that allows Mtb to tolerate a more prolonged exposure to acidic conditions [100].

Notably, even the modest degree of phagosomal acidification that occurs during Mtb infection plays an important role in successful host colonization. When phagosomal acidification was inhibited using concanamycin A, Mtb lost a substantial portion of the transcriptional response normally induced during macrophage infection, indicating that acidic pH functions as a key environmental cue [101]. Indeed, bacteria residing within phagosomes exhibit distinct transcriptional profiles that shape both metabolic activity and interactions with the host immune response [38]. A key mediator of the transcriptional adaptation of Mtb to acidic pH is the PhoPR TCS, which consists of the sensor HK PhoR and the RR PhoP. The PhoPR TCS regulates genes that are essential for acid stress adaptation and blocking phagosomal acidification prevents their induction [59, 101]. Importantly, deletion of *phoP* markedly impaired the ability of Mtb to colonize macrophages and to establish infection in murine models [22]. This attenuation was so pronounced that *phoP*-deficient strains have been explored as the basis for live attenuated vaccine candidates [102]. Although acidic pH alone triggers a broad range of bacterial responses, it rarely acts in isolation. Proton fluxes are typically coupled to the movement of counterions, meaning that pH changes occur alongside shifts in ionic composition. Consequently, Mtb likely interprets acidification as part of a composite environmental signal, integrating pH with other host-derived cues to fine-tune its adaptive responses.

1.2.4: Chloride (Cl^-)

Acidic pH has been long recognized as a key environmental signal encountered by Mtb during infection, but chloride (Cl^-), the most abundant anion in the human body, has become increasingly characterized as a physiologically relevant cue [103]. In host cells, Cl^- plays a central role in maintaining osmolarity, intracellular pH, and membrane potential [104]. These processes are largely mediated by Cl^--specific transporters that often function through H^+ exchange [105, 106]. Appropriate host immune cell function relies on Cl^- signaling, particularly within phagosomes [105] and endosomes [107]. In neutrophils, Cl^- functions as a substrate for myeloperoxidase, which converts hydrogen peroxide and Cl^- into hypochlorous acid and other reactive antimicrobial species [108]. Of particular importance regarding Mtb infection, Cl^- acts as a counterion in the process of macrophage phagosomal acidification, resulting in the simultaneous exposure of engulfed Mtb to acidic pH and elevated Cl^- concentrations [109]. Consistent with this host environment, phagosomal acidification has been shown to be correlated with Cl^- accumulation [59]; blocking acidification with the vacuolar proton pump inhibitor bafilomycin A1 consequently also blocks Cl^- accumulation [59].

When Mtb is exposed to elevated environmental Cl^- levels, the bacterium mounts a robust transcriptional response that increases in a concentration-dependent manner [59]. Notably, there is substantial overlap between genes induced by high environmental Cl^- levels and those induced by acidic pH, indicating that these signals are at least partially integrated at the transcriptional level [59]. Further, it has been shown that the response to acidic pH and high [Cl^-] is synergistic [59]. Indeed, it was found that the PhoPR TCS also plays a significant role in the regulation of the bacterium's transcriptional response to Cl^-,

as it does for acidic pH, with disruption of *phoPR* diminishing the response to elevated Cl^- and abolishing the response to acidic pH alone [59]. However, the synergistic transcriptional response to the combined presence of both signals is not completely lost, suggesting that additional regulatory pathways work to enable Mtb to sense and coordinate its response to multiple environmental cues concurrently, a concept that is the basis for the questions pursued in my thesis work.

1.2.5: Potassium (K^+)

While Cl^- is the most abundant anion in the human body, potassium (K^+) functions as the predominant intracellular cation in mammalian cells, maintained at concentrations of approximately 140-150 mM [110]. In eukaryotic systems, K^+ gradients underpin a wide range of essential processes, including neuronal signaling [111], muscle contraction [112], and epithelial hydration and clearance [113]. Like Cl^-, cellular K^+ homeostasis is tightly regulated by dedicated transporters and pumps [114]. Beyond its structural and metabolic roles, K^+ is a key regulator of host immune function [115]. For instance, alveolar macrophages require K^+ for proper immune response [116]. Another well-characterized example of the role of K^+ in host immunity is in the activation of the NLRP3 inflammasome, which is triggered by K^+ efflux from the cytosol following cellular stress or pathogen detection [117]. At the host-pathogen interface, dynamic changes in K^+ are also evident within phagosomes where it has been shown that K^+ accumulates during macrophage phagosome maturation, indicating that pathogens are exposed to a K^+-rich environment [60].

In pathogenic bacteria, environmental K^+ can function as a regulatory signal that influences virulence. For example, *Salmonella enterica* upregulates virulence gene expression in response to elevated K^+ levels [118, 119], and disruption of K^+ uptake systems impair pathogenicity in diverse organisms including *Staphylococcus aureus* [120] and Mtb [60]. In Mtb, K^+ acquisition and sensing are mediated by multiple transport and regulatory mechanisms, underscoring the importance of K^+ homeostasis during infection. The Trk system is a major, constitutive K^+ uptake pathway and disruption of Trk function results in significant attenuation of Mtb *in vivo* [60]. Perturbation of K^+ balance leads to widespread transcriptional remodeling, particularly affecting genes involved in ion transport and stress adaptation [60]. Mtb encodes the KdpDE TCS, a conserved signal transduction pathway that senses K^+ limitation and induces expression of the high-affinity KdpFABC transporter [121]. KdpDE thus enables Mtb to respond to changes in K^+, particularly in conditions in which K^+ is limiting or where ionic stress is compounded by other environmental pressures encountered in the host.

1.3: Bacterial environmental sensing through signal transduction regulatory mechanisms

1.3.1: Two-component systems (TCSs) and transcriptional regulation in response to environmental signals

Bacteria rely on sophisticated signal transduction mechanisms to sense and adapt to rapidly changing environmental conditions [122, 123]. Among these signaling mechanisms, TCSs represent one of the most highly studied strategies for coupling

environmental sensing and transcriptional regulation [122-126]. TCSs are typically comprised of a sensor HK that detects a specific stimulus and a cognate RR that modulates gene expression following phosphotransfer from the HK [122, 123, 125]. Critically, studies across diverse bacterial species have demonstrated that TCSs govern processes essential for survival including nutrient acquisition [127], osmotic balance [128], and virulence [129-131]. For example, in *E.coli*, the EnvZ/OmpR system provides a canonical example of osmotic sensing. Changes in environmental osmolarity alter the HK EnvZ autophosphorylation activity [132], consequently leading to differential phosphorylation of the OmpR RR [128]. Deletion of *ompR* or introduction of phosphomimetic mutations result in aberrant porin expression and impaired growth under osmotic stress [133, 134]. Similarly, the PhoR/PhoB system in *E. coli* responds to phosphate limitation, with chromatin immunoprecipitation (ChIP) and reporter assays demonstrating PhoB binding to the conserved PHO box sequences upstream of genes involved in phosphate uptake and metabolism [127]. Loss of *phoB* results in a severe growth defect in phosphate-limited media, underscoring the adaptive value of this regulation [127].

TCSs also play a central role in regulating bacterial pathogenicity and virulence. In *S. enterica*, the PhoP/PhoQ system (distinct from the PhoPR TCS in Mtb) senses low Mg^{+}, acidic pH, and antimicrobial peptides, signals that are characteristic of the macrophage phagosome [135]. Transcriptomic analyses revealed that the PhoP RR regulates hundreds of genes involved in lipid A modification [136], resistance to host defenses, and intracellular survival [137]. Mutants lacking *phoP* or *phoQ* are found to be attenuated in murine infection models providing further evidence for the necessity of

appropriate bacterial sensing in the success of bacterial virulence [129]. Likewise, in *Vibrio cholerae*, the ToxR/ToxS system regulates expression of cholera toxin and toxin-coregulated pili [130, 138]. Deletion of *toxR* abolishes virulence gene expression and renders bacteria avirulent in infant murine models [130, 138]. Together, these examples demonstrate how TCS-mediated transcriptional regulation can be essential for driving disease progression during infections by bacterial pathogens.

The Mtb genome encodes a relatively limited number of TCSs (12) compared to free-living bacteria, yet genetic and functional studies indicate that these systems are central to pathogenesis and persistence [124, 139]. As described, Mtb encounters a complex and dynamic array of environmental stresses. While many of these signals are experienced during its intracellular residence, such as acidic pH, hypoxia, NO, high [Cl^-], and changes in [K^+], Mtb populations also occupy extracellular niches where reduced oxygen tension, nutrient limitation, and altered host-derived signals predominate. TCSs enable Mtb to sense cues across both intracellular and extracellular host environments, translating those signals into appropriate transcriptional responses.

One of the most well characterized TCSs in Mtb, as well as the focus of much of my thesis work, is the DosRS(T) TCS. As introduced above, DosRS(T) serves as the primary regulator of the transcriptional response of Mtb to hypoxia and NO [65, 66]. Activation of the DosR RR leads to induction of the dormancy regulon, comprised of 48 genes, that supports physiological transitions associated with reduced replication and persistence [66, 75]. Genetic studies underscore the functional importance of this pathway in Mtb survival under stress. It has been shown that deletion of *dosR* abolished induction of the dormancy regulon and reduced bacterial survival under hypoxic

conditions *in vitro* [39, 73]. Supporting a role for the DosRS(T)-mediated regulon during chronic infection, experiments performed in a macaque model of infection showed that a Δ*dosR* Mtb mutant is reduced in its ability to replicate as compared to WT Mtb, exhibiting significantly reduced growth in lung tissue [66, 75]. The ability of Mtb to fine-tune its transcriptional response to redox stress is exhibited by work performed by Wayne and Hayes [34]. The expression of *dosRS* and *dosT* themselves are induced by NO and hypoxia, and experimental data generated by this group indicated the graded induction of the regulon in response to varying oxygen levels [140]. The ability of DosR to modulate its transcriptional response to environmental stress in a context-dependent manner is a key concept that will be expanded upon throughout this thesis work.

The PrrAB TCS adds an additional layer of regulatory complexity to Mtb by linking environmental sensing to central metabolism and respiratory function. PrrAB is homologous to the RegBA/PrrBA systems characterized in other actinomycetes and proteobacteria [141], where it functions as a redox-responsive regulator of energy metabolism [142]. In Mtb, PrrAB is required for optimal growth and survival, and because this system is essential, its function has been interrogated through conditional depletion or partial loss-of-function approaches rather than deletion [142, 143]. These perturbations result in widespread transcriptional remodeling, particularly affecting genes involved in respiration, electron transport, and metabolic flux [142]. Additionally, work in our lab has shown that PrrA functions in the regulation of Mtb response to acidic pH, Cl^-, NO, and hypoxia, acting as a "master" modulator of the bacterium's response to its environment [143]. Notably, PrrAB-regulated genes partially overlap with those controlled by both the DosRS(T) and PhoPR TCSs, indicating that Mtb employs multiple,

interconnected TCSs to fine-tune physiological adaptation under changing environmental conditions [144, 145].

PhoPR represents another major regulatory system in Mtb with broad transcriptional influence. As noted above, PhoPR is central to acidic pH/Cl^--responsive regulation and virulence [131]. Beyond this role, RNA-seq and ChIP-seq studies have expanded the known PhoP regulon to include genes involved in lipid biosynthesis, secretion systems including ESX-1, and cell envelope composition [146, 147]. These findings highlight that PhoPR coordinates not only stress adaptation, but also structural and secretory pathways that shape host-pathogen interactions.

Additional TCSs highlight the importance of signal integration for successful Mtb survival and infection. Consistent with its role in K^+ homeostasis described above, KdpDE is required for optimal adaptation to K^+-limiting environments [148]. Loss of KdpDE compromises bacterial growth specifically under low K^+ conditions and is accompanied by altered expression of stress-associated genes [148], reinforcing that this system contributes not only to K^+ acquisition but also to broader adaptive responses to ionic stress.

Collectively, experimental data from diverse bacterial species demonstrate the indispensability of TCSs in translating environmental signals into adaptive transcriptional responses for bacterial survival. Importantly, these systems are not isolated switches, but components of interconnected regulatory networks that integrate multiple, simultaneous cues encountered within the host. This capacity for signal integration and transcriptional coordination is fundamental for the ability of Mtb to persist, evade host immune defenses, and cause chronic disease.

1.3.2: Serine/threonine protein kinases (STPKs) and post-translational modification in response to environmental signals

Bacterial adaptation to dynamic environmental conditions depends not only on transcriptional-level regulation, but also on rapid, reversible post-translational mechanisms that can directly modulate protein activity. Among these, serine/threonine protein kinases (STPKs) have emerged as key regulators of cellular physiology across diverse bacterial taxa [149]. Once thought to be largely restricted to eukaryotic systems and less widely distributed among different groups of bacteria, STPKs are now recognized as widespread across bacterial species, where they provide an additional layer of signal integration and response distinct from, yet complementary to, transcriptional regulatory systems such as TCSs [149, 150].

Bacterial STPKs are classically Hanks-type kinases that share structural and catalytic features with their eukaryotic counterparts, including conserved motifs required for ATP binding and phosphotransfer [151]. Across bacterial species, these kinases catalyze the phosphorylation of serine and threonine residues on target proteins, thereby modulating enzymatic activity, protein-protein interactions, subcellular localization, or stability [152-157]. Unlike TCSs, rather than having a cognate partner, a given STPK instead phosphorylates many targets.

Studies across bacterial species demonstrate the importance of STPK-mediated regulation on fundamental aspects of cell physiology. In *Bacillus subtilis*, for example, the STPK PrkC senses extracellular muropeptides released during cell wall remodeling and germination [158]. Importantly, activation of PrkC through binding of muropeptides to the extracellular PASTA domains plays a key role in regulating substrates involved in

translation and cell growth [158]. Similarly, in *Streptococcus pneumoniae*, the STPK StkP regulates cell division by phosphorylating DivIVA and other substrates involved in septum formation [152, 153]. STPKs have also been strongly implicated in bacterial pathogenicity and stress response. The PrkA kinase in *Listeria monocytogenes* responds to cell envelope stress and controls phosphorylation of ReoM, a critical intermediate in the activation of MurA involved in peptidoglycan synthesis [154]. Mutants lacking *prkA* display heightened sensitivity to antibiotics targeting the cell wall and reduced survival within host cells [159]. Together, these data highlight the ability of STPKs to rapidly reprogram bacterial physiology in response to extracellular and intracellular stress signals.

In Mtb, STPKs play a significant role in environmental sensing and adaptation, reflecting the bacterium's prolonged residence within the hostile and heterogenous host environment of the macrophage and phagolysosome. While most bacterial genomes encode one or two STPKs, the Mtb genome encodes 11 STPKs, some of which have been shown to be important for successful bacterial growth and virulence [155]. For example, PknA and PknB are essential kinases that coordinate cell growth and division in response to changes in cell envelope status [155]. Similar to the STPK-mediated activation of PrkC in *B. subtilis*, PknB contains extracellular PASTA domains that bind peptidoglycan fragments, providing a direct mechanism for sensing cell wall remodeling [156]. Further, activation of PknB leads to phosphorylation of substrates involved in peptidoglycan synthesis and polar growth, including Wag31 [157]. Inhibition or depletion of PknA or PknB in Mtb results in severe morphological defects and loss of viability, further implicating these kinases in maintaining growth control [160].

Critically, many Mtb STPKs function in the sensing of environmental stressors as well as integration of these stressor signals. A key STPK that is the focus of much of this thesis work is PknH. PknH has been implicated in regulating the composition of the Mtb cell envelope as well as virulence-associated pathways [161]. Although a functional PknH is not essential for growth *in vitro* [162], transcriptomic analyses of a *pknH* deletion mutant strain revealed altered expression of genes involved in lipid metabolism, cell wall biosynthesis, and stress responses, consistent with defects in envelope homeostasis [161]. Further biochemical and phosphoproteomic studies provide direct evidence that PknH regulates envelope-associated pathways at the post-translational level [161]. For example, PknH phosphorylates the transcriptional regulator EmbR, enhancing its DNA-binding activity and promoting expression of the *embCAB* operon, which encodes arabinosyltransferases required for cell wall arabinan synthesis [163-165]. Despite these molecular effects, *pknH*-deficient Mtb exhibits a higher bacterial load in a chronic murine infection model, indicating that PknH-dependent regulation also influences *in vivo* host-pathogen interactions [162]. These findings suggest that PknH can act as a key integrator of environmental signals contributing to Mtb adaptation and virulence.

Another STPK of particular interest in this thesis work is PknD, which functions as a sensor of extracellular environmental cues, including osmotic stress [166]. Under osmotic stress, a Mtb *pknD* mutant exhibited altered levels of key proteins involved in cell envelope integrity and stress adaptation, consistent with defective signal transduction [166]. Further, loss of *pknD* resulted in attenuated dissemination and altered tissue pathology *in vivo*, further supporting the conclusion that PknD-mediated sensing of

extracellular osmotic conditions contributes to early host interaction and virulence [167]. Collectively, STPKs provide bacterial species with a rapid, flexible, and highly interconnected signaling platform that complements transcriptional regulation. Through these kinases, pathogens such as Mtb can sense diverse environmental cues and translate them into coordinated physiological responses that support survival, persistence, and pathogenicity within the host.

1.4: Integration of TCSs and STPKs

1.4.1: Interplay between TCSs and STPKs across bacterial species

A growing body of experimental evidence demonstrates that canonical TCSs and STPKs do not act alone in regulatory signal transduction, but instead physically and functionally cooperate to coordinate bacterial response to a multitude of environmental signals. Indeed, it has been increasingly shown that there is direct modification of TCS components or their downstream effectors by STPKs, thereby fine-tuning transcriptional outputs [150, 154, 159, 168, 169]. Phosphorylation of regulatory proteins like TCSs allow for the integration of environmental information across regulatory layers, enabling Mtb to coordinate immediate post-translational responses with long-term transcriptional reprogramming.

A direct example of this interplay can be found in *B. subtilis* where *in vitro* kinase assays demonstrated the direct phosphorylation of the response regulator WalR, part of the essential TCS WalKR, by the STPK PrkC [168]. The importance of this phosphorylation is demonstrated by electrophoretic mobility shift assays (EMSAs) in which loss of PrkC-mediated phosphorylation resulted in defective WalR-dependent gene

expression and altered cell envelope homeostasis [168]. In *Streptococcus pyogenes*, phosphoproteomic mapping and transcriptional reporter assays demonstrated that the STPK Stk phosphorylates the CovR response regulator of the CovRS TCS [169]. Further, phosphoablative mutations at STPK phosphorylation sites reduced CovR-dependent repression of virulence genes, leading to hypervirulence in murine infection models [169]. As mentioned above, in *L. monocytogenes*, the kinase PrkA phosphorylates the TCS-associated regulator ReoM, affecting cell wall stress responses and conferring susceptibility to β-lactam antibiotics when *prkA* is mutated [154, 159]. Collectively, these examples across bacterial species reveal that TCS components, including both HKs and RRs, are targets of STPKs. This integration expands the traditional view of bacterial signaling, illustrating a phosphorylation network that enables nuanced, adaptive responses across a multitude of environmental contexts.

1.4.2: Evidence of TCS-STPK interplay in Mtb

In Mtb, it has become more widely accepted that STPKs directly engage with TCSs, adding a previously underappreciated layer of regulatory complexity to environmental signal integration. Indeed, this was made evident when global mass spectrometry-based phosphoproteomic profiling revealed extensive *O*-phosphorylation on both HKs and RRs of all 12 TCSs encoded by Mtb, identifying more than 170 distinct STPK phosphorylation sites across the TCS signaling network and implicating multiple STPKs as potential upstream regulators of TCS activity [150].

Additional studies in Mtb specifically highlight the extensive intersections between STPKs and TCS RRs specifically at the level of environmental cue integration.

Using biochemical assays with purified proteins, previously published research has demonstrated an *in vitro* interaction between the STPK PknH and the DosR RR [170]. Our lab has found further evidence for the coordination between STPKs and TCSs in response to environmental signals, specifically through the STPK regulation of the RR PrrA [143]. Strikingly, we have shown that a STPK phosphoablative PrrA mutation (T6A) resulted in increased growth of Mtb in broth culture, significant alteration in the bacterium's transcriptional response to acidic pH and high [Cl^-], and decreased environmental response to both NO and hypoxia [143]. Further, the PrrA T6A Mtb mutant was incapable of entry into an adaptive state of growth arrest upon extended exposure to NO and attenuated for colonization *in vivo* [143]. While there is clear evidence for interplay between STPKs and TCSs, there remains much to be understood regarding how these two signal transduction regulatory mechanisms interact in the coordination of Mtb environmental adaptation.

1.5: Thesis overview

Collectively, these studies demonstrate that STPKs in Mtb are not isolated signaling entities but instead form a layered regulatory network with TCSs, where post-translational modification of HKs and RRs fine-tune gene expression in response to the varied environmental cutes encountered during infection. This integration enhances both the specificity and flexibility of the adaptive response of Mtb, providing a mechanistic basis for its persistence and pathogenicity in host tissues. My thesis research thus aimed to define specific interactions between STPKs and TCSs, and to understand how this

interplay modulates Mtb growth in response to the major environmental cues encountered during host infection.

Chapter 2: Serine/threonine protein kinase phosphorylation of DosR alters target gene transcription mechanics and regulates *Mycobacterium tuberculosis* response to nitric oxide stress

Sontag NR, Ruiz Manzano A, Ecker AMV, Galburt EA, Tan S. (2026) Serine/threonine protein kinase phosphorylation of DosR alters target gene transcription mechanics and regulates *Mycobacterium tuberculosis* response to nitric oxide stress. PLoS Genetics 22(2): e1012043. doi: 10.1371/journal.pgen.1012043.

2.1 Introduction

The ability of *Mycobacterium tuberculosis* (Mtb) to sense and respond to dynamic changes in environmental signals encountered throughout the course of infection is critical for successful host colonization. This includes cues such as acidic pH, chloride (Cl^-), potassium (K^+), nitric oxide (NO), and hypoxia, which are associated with the host immune response [39, 59, 60, 77, 101, 171, 172]. Mtb is the causative agent of tuberculosis and is the leading global cause of death from an infectious disease [13]. The heterogeneity of the environment Mtb experiences during host infection further affects the bacterial physiological state and contributes importantly to the difficulty of tuberculosis treatment [173-177].

Phosphorylation-based signal transduction enables environmental adaptation by linking extracellular signals to intracellular regulatory mechanisms. In bacteria, the best-studied mechanism of phosphorylation-based transmembrane signaling are two-component systems (TCSs), where ligand binding by the transmembrane histidine kinase (HK) sensor protein initiates a phosphorelay to the cognate intracellular response regulator (RR) protein, canonically a transcription factor that controls expression of specific genes [178, 179]. The number of TCSs per bacterial genome strongly correlates with ecological and environmental niche [180, 181] - bacteria living in more constant environments usually encode fewer TCSs, while bacteria that inhabit rapidly changing or diverse environments typically encode larger numbers of these signaling proteins that are critical for cellular processes [182-184]. Mtb encodes 12 TCSs that play a key role in virulence, environmental adaptation, and infection [178]. For example, inactivation of PhoPR, a key TCS involved in Mtb response to acidic pH and Cl^- [59, 101], results in

significant attenuation in the ability of Mtb to colonize its host [131]. An essential TCS in Mtb, PrrAB, was reported to be involved in early adaptation to intracellular infection [142, 185], and we have since shown that PrrA is a global regulator of Mtb response to acidic pH, high [Cl^-], hypoxia and NO [143]. The TCS DosRS(T) regulates Mtb response to hypoxia and NO, and upon sensing of these signals, mediates induction of a "dormant" state through the control of 48 genes known as the "dormancy regulon" [39, 65, 77, 172]. The TCS KdpDE is responsible for regulation of the Kdp K^+ uptake system and is pivotal for Mtb adaptation to low environmental potassium levels ([K^+]) [60, 121]. These examples illustrate the importance of TCSs for Mtb adaptation to its local environment.

Importantly, in addition to TCSs, signal transduction and environmental response in Mtb is also mediated by serine/threonine protein kinases (STPKs) [186-188]. In contrast to TCSs, STPKs have a larger set of phosphorylation targets, and while STPKs are often less numerous in the genome of a given bacterium, their widespread presence and impact on bacterial biology have become increasingly appreciated [150, 186-190]. For example, phosphorylation of glutamyl tRNA reductase by the STPK Stk1 plays an important role in the regulation of heme biosynthesis in *Staphylococcus aureus* [191]. Another example is with *L. monocytogenes*, where phosphorylation of the protein ReoM by the STPK PrkA is essential for viability, due to its role in peptidoglycan synthesis [154]. The Mtb genome markedly contains a comparatively large number of STPKs compared to other bacterial species, with 11 STPKs encoded [186, 189, 192]. Notably, global phosphoproteome studies have identified TCS RRs as potential substrates of STPK phosphorylation [150, 190], raising the concept of STPK-TCS interplay in the regulation of TCS function. Indeed, there is increasing support for this interplay, with

studies in bacterial species ranging from Mtb and *Bordetella*, to *Streptococcus pneumoniae*, *S. aureus*, and *Bacillus subtilis* [150, 168, 170, 190, 193-197]. Specifically for Mtb, all 12 TCS RRs have been identified from global phosphoproteome studies as potential substrates of STPK phosphorylation [150, 190]. In the case of DosR and PrrA, both RRs from TCSs that respond to NO stress among other signals, biochemical assays with purified proteins have further verified their phosphorylation by STPKs [170, 198], with the STPK PknH shown to phosphorylate DosR [170]. Strikingly, we have shown that a STPK phosphoablative PrrA-T6A Mtb mutant was significantly altered in its transcriptional response to acidic pH and high [Cl^-], and dampened in environmental response to both NO and hypoxia [143]. Consequently, this mutant was incapable of entry into an adaptive state of growth arrest upon extended exposure to NO and attenuated for host colonization *in vivo* [143]. While there is clear evidence for interplay between STPKs and TCSs, much remains unknown regarding how the two systems interact in the coordination of Mtb environmental adaptation.

Here, we examined STPK interactions with the RRs DosR, PrrA, PhoP, and KdpE, all RRs known to play critical roles in Mtb transcriptional response to environmental cues encountered throughout host infection [39, 59, 60, 77, 101, 172], revealing both specificity and overlap in interactions. Focusing on DosR as an exemplar system, we find that PknH and PknD phosphorylation of purified DosR decreased its binding to the promoter of its target genes, with strong binding restored by combined treatment with acetyl phosphate (AcP), which mimics HK phosphotransfer [199, 200]. Further, PknH and PknD phosphorylation of purified DosR decreased the steady-state transcription rate of DosR target genes, in contrast to the increase observed upon AcP

treatment of DosR. Additionally, STPK phosphorylation shifted the AcP-treated DosR concentration-dependence of target gene activation. Finally, we found that a Δ*pknH* Mtb mutant exhibited increased DosR regulon transcription at lower NO levels than wild type (WT) Mtb. Combined, our work sheds light on the mechanisms underpinning STPK-TCS interplay, illustrating how STPK phosphorylation of a TCS RR can act to restrain its activation to ensure response initiation only when appropriate.

2.2 Results

2.2.1 There is both overlap and specificity in interactions between STPKs and TCS RRs

To systematically identify possible interactions between STPKs and TCSs RRs, we utilized the mycobacterial protein fragment complementation (M-PFC) assay [201]. Comparable to the bacterial two-hybrid assay, this method is based on functional reconstitution of the murine dihydrofolate reductase (mDHFR) driven by interactions between two test proteins, thereby conferring resistance to trimethoprim (TRIM) [201]. A previous study applying this method uncovered an interaction between DosR and the STPK PknH, providing precedence for its use in this context [170]. In particular, we examined the RRs DosR, PrrA, PhoP, and KdpE, fusing the open reading frame of each to the mDHFR fragment F1,2, with each of 9 STPKs fused to the mDHFR fragment F3. Some combinations of RRs and specific STPKs showed clear growth at 50 μg/mL TRIM, indicating a strong interaction (Figs 2.1 and 4.1). As controls, *Mycobacterium smegmatis* containing empty vectors were unable to grow on 7H10 TRIM plates, whereas all strains

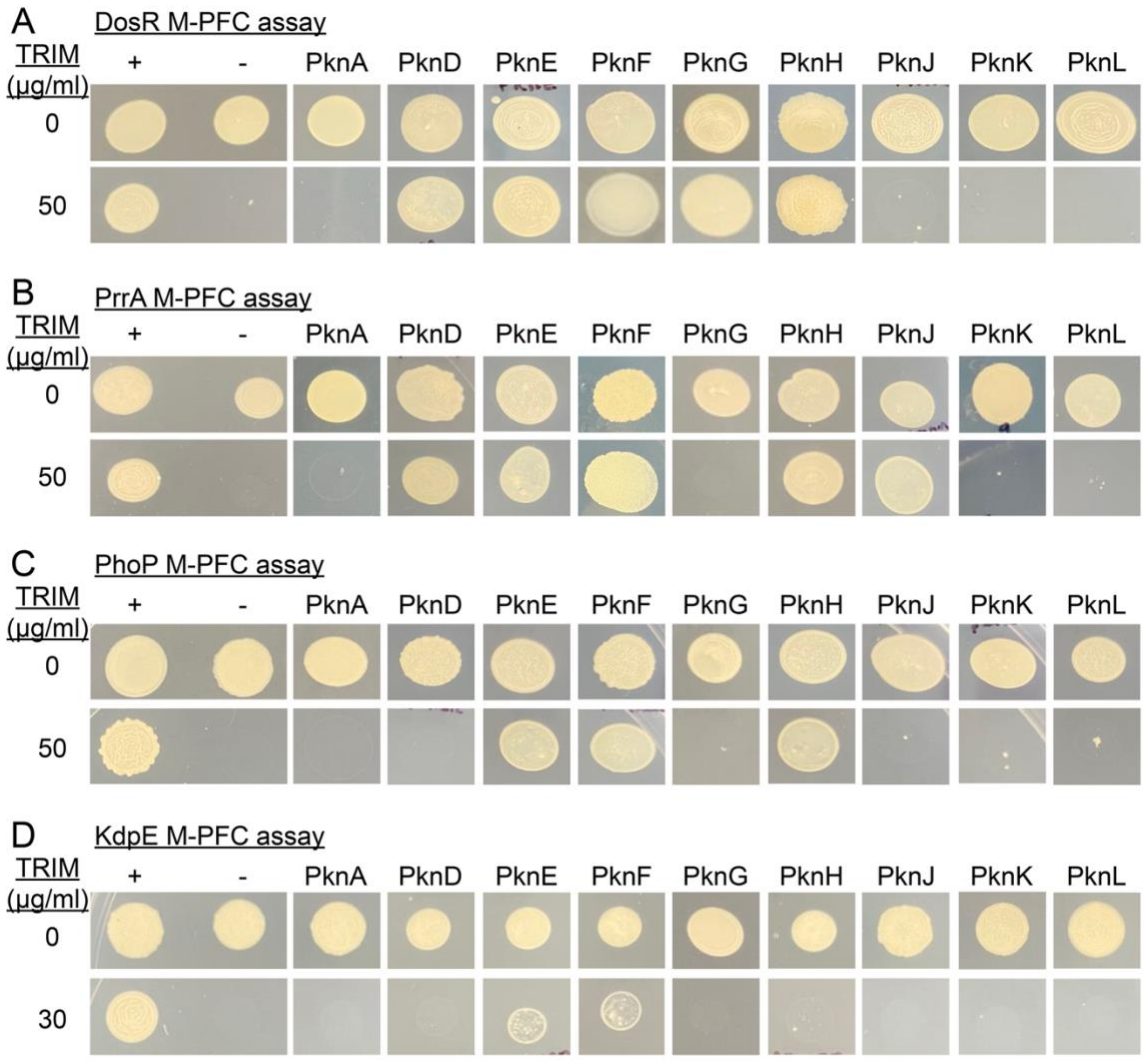

Figure 2.1. Specificity of interactions between TCS RRs and STPKs. Interactions between the TCS RRs DosR (A), PrrA (B), PhoP (C), or KdpE (D) with the various STPKs (kinase domains only for all except PknG and PknK) were tested by M-PFC assay. The positive control ("+") was *M. smegmatis* expressing the *S. cerevisiae* GCN4 dimerization domains fused to the F1,2 or F3 domains of the murine dihydrofolate reductase gene; the negative control ("-") was *M. smegmatis* expressing the respective RR fused to the F1,2 domain and a F3 domain that was not fused to any Mtb gene. Data are representative of 3 independent experiments.

grew well on 7H10 plates lacking TRIM (Fig 2.1). We compared interactions across four RRs to explore possible relationships between environmental signals responded to by a TCS and interactions with STPKs, as shown in Fig. 4.1. Interestingly, we observed

almost complete overlap in the STPKs that interact with PrrA and DosR, with smaller subsets of those same STPKs interacting with PhoP and KdpE. These results indicate that there is both overlap and specificity in the interactions between STPKs and RRs.

In accord with previous results [170], mass spectrometry (MS) analysis of recombinantly expressed and purified DosR that was subsequently phosphorylated *in vitro* with recombinant PknH identified phosphorylation at the Thr198 and Thr205 residues (Figs 4.2-4.4). Analysis of DosR samples also directly confirmed that AcP treatment, mimicking HK phosphotransfer [199, 200], led to phosphorylation of the Asp54 residue (Fig 4.5) [202, 203]. Notably, analyzing the results from a previous global study of the Mtb *O*-phosphoproteome, where phosphosites in individual STPK overexpression and deletion mutants were compared to WT Mtb [150], provided support for the likely physiological interactions of several STPK-TCS RRs indicated by our M-PFC assay results. In particular, significant differences in phosphopeptides within DosR (*i.e.*, increased presence upon STPK overexpression and/or decreased presence with the STPK deletion mutant, as compared to WT Mtb) were identified for all of the STPKs identified as DosR interactors in our M-PFC assay [150]. This was similarly the case for PhoP, while significant differences in phosphopeptides within PrrA were identified for PknD and PknE in the global phosphoproteome study [150]. Together, our results reinforce the concept of extensive interplay between STPKs and TCS RRs in Mtb.

2.2.2 Changes in DosR phosphorylation status alter its binding affinity to target promoters

TCS RRs are canonically transcription factors that mediate their activity through changes in gene transcription [178, 179]. To examine how STPK phosphorylation of TCS RRs mechanistically affect their function, we thus first analyzed effects on target promoter binding, focusing our studies on DosR as an exemplar RR. As expected, AcP treatment to mimic HK phosphotransfer enhanced DosR binding to the promoter of *hspX*, a member of the DosR regulon [39, 65, 199], as indicated by electrophoretic mobility shifts observed at lower DosR concentrations with AcP-treated DosR (Fig 2.2A, 2.2B, quantified in 2.2G). Intriguingly, *in vitro* phosphorylation of DosR with the STPK PknH or PknD resulted in decreased DNA binding affinity to a similar degree (compare Fig 2.2C and 2.2D to 2.2A, quantified in 2.2G). In a live bacterium, both HK phosphotransfer and STPK phosphorylation might be expected to co-occur at times, therefore we next examined the influence of both types of phosphorylation on DosR target promoter binding affinity. AcP treatment of PknH or PknD phosphorylated DosR resulted in a DNA binding affinity that resembled that of AcP-treated DosR alone (compare Fig 2.2E and 2.2F to 2.2B, quantified in 2.2G). Similar changes in promoter binding affinity depending on DosR phosphorylation status were observed with DosR binding to the promoter of *fdxA*, another member of the DosR regulon (Fig 4.6) [39, 65, 204]. For both the *hspX* and *fdxA* promoters, competition experiments with unlabeled probes of each respective promoter reversed the gel shift in a concentration-dependent manner (Figs 4.7A and 4.7B). Conversely, competition experiments with an unlabeled probe of a promoter not bound by DosR (*rv2390c* promoter [60]) did not affect the gel shift (Figs 4.7C and 4.7D). These results demonstrate the specificity of the binding results.

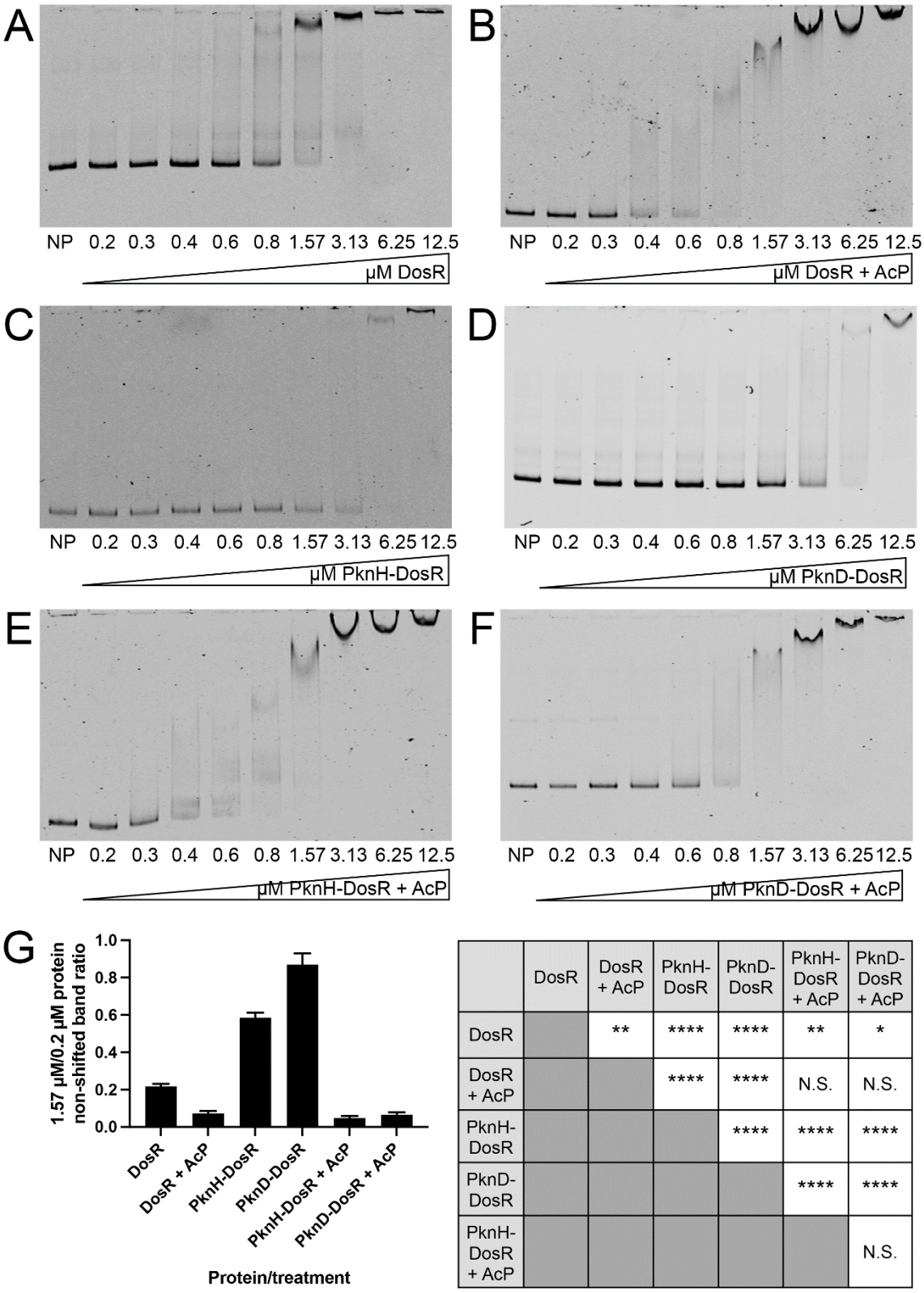

	DosR	DosR + AcP	PknH-DosR	PknD-DosR	PknH-DosR + AcP	PknD-DosR + AcP
DosR		**	****	****	**	*
DosR + AcP			****	****	N.S.	N.S.
PknH-DosR				****	****	****
PknD-DosR					****	****
PknH-DosR + AcP						N.S.

Figure 2.2. Changes in DosR phosphorylation status alter binding affinity to the promoter of its target gene *hspX*. Electrophoretic mobility shift assays (EMSAs) using

purified recombinant C-terminally 6x-His-tagged DosR and IRDye 700-labeled probes for the *hspX* promoter are shown. A control with no protein ("NP") added is shown for each gel. DosR was added at indicated concentrations for all other lanes. 40 fmoles of *hspX* promoter DNA was used in each reaction. EMSAs shown are as follows: (A) untreated DosR, (B) DosR incubated with 50 mM acetyl phosphate (AcP), (C) DosR phosphorylated "on-bead" with 1 μM PknH, (D) DosR phosphorylated "on-bead" with 1 μM PknD, (E) DosR phosphorylated "on-bead" with 1 μM PknH, then purified and incubated with 50 mM AcP, and (F) DosR phosphorylated "on-bead" with 1 μM PknD, then purified and incubated with 50 mM AcP. Data are representative of at least 3 independent experiments. Quantification of the intensity of the non-shifted band in the 1.57 μM protein EMSA reaction versus that in the 0.2 μM reaction for each protein/treatment is shown in (G). Data are shown as means ± SEM from 3-5 experiments. p-values shown in the table on the right in panel (G) were obtained with a one-way ANOVA with Tukey's multiple comparisons. N.S. not significant, * $p<0.05$, ** $p<0.01$, **** $p<0.0001$. The numerical data underlying the graph shown in this figure are provided in Data File 4.1.

Complementary to the electrophoretic mobility shift assays (EMSAs), we utilized fluorescence polarization to further quantitatively measure DosR binding to target gene promoters. Consistent with the EMSA results, the dissociation constant (K_d) of DosR binding to its target *hspX* and *fdxA* promoters was significantly increased upon PknH or PknD phosphorylation of DosR, demonstrating a decrease in binding affinity (Fig 2.3). Together, these results show that STPK phosphorylation of DosR alone, in the absence of HK phosphotransfer, decreases the affinity of DosR for its target gene promoters, indicating that STPK phosphorylation can serve as a modulatory mechanism providing tighter control of DosR activation.

2.2.3 STPK phosphorylation of purified DosR decreases the level and alters concentration-dependence of steady-state transcription rates of its target genes

While EMSAs and fluorescence polarization assays provide insight into target promoter DNA binding, RR promoter binding affinity is just one factor determining its

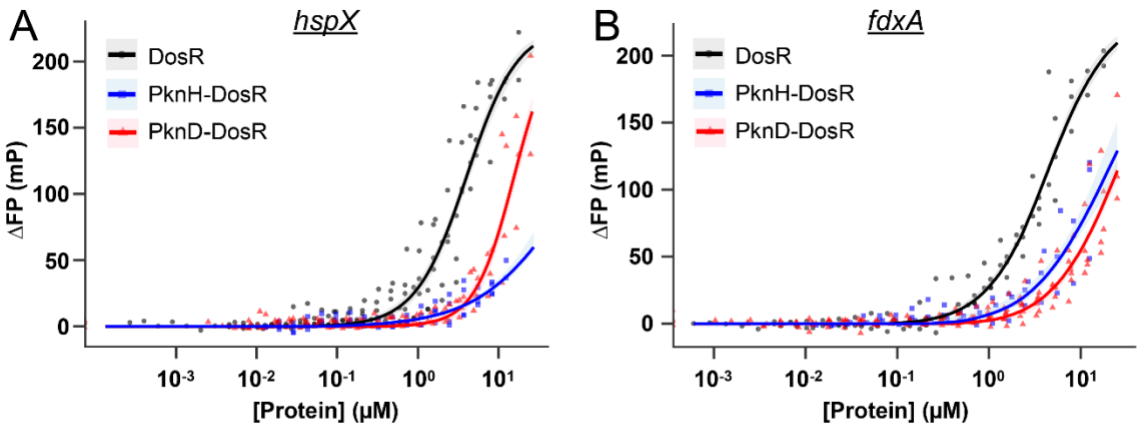

DosR	PknH-DosR	PknD-DosR
K_d = 3.8 ± 0.2	K_d = 95.0 ± 29.1	K_d = 15.0 ± 0.6
n = 1.4 ± 0.1	n = 0.8 ± 0.1	n = 1.8 ± 0.1

DosR	PknH-DosR	PknD-DosR
K_d = 4.4 ± 0.2	K_d = 19.8 ± 3.1	K_d = 25.6 ± 1.4
n = 1.3 ± 0.1	n = 1.0 ± 0.1	n = 1.2 ± 0.1

Figure 2.3. Fluorescence polarization assays demonstrate inhibition of DosR binding to its target gene promoters upon PknH or PknD phosphorylation. The change in fluorescence anisotropy (ΔFP) relative to no protein was measured as a function of increasing concentrations of DosR (black curves), PknH-phosphorylated DosR (blue curves), or PknD-phosphorylated DosR (red curves) incubated with a fluorescently labeled *hspX* (A) or *fdxA* (B) promoter DNA region. The fit using a Hill equation to estimate binding parameters with 95% confidence intervals (shaded regions) are shown. The dissociation constants (K_d) and Hill coefficients (n) are indicated in the tables below the graphs.

effect on gene transcription. For example, a transcription factor with high DNA-binding affinity but with reduced ability to interact productively with RNA polymerase [205, 206], or to modulate the kinetics of transcription initiation [207], would not be expected to be a strong transcriptional activator. To investigate the effects of STPK phosphorylation on RNA production directly, we utilized a fluorescent RNA aptamer-based method to quantify the effect of STPK phosphorylation of purified DosR on the steady-state rate of target gene transcription. This assay exploits the use of a Spinach-mini aptamer that produces a fluorescence-based enhancement when binding a small molecule fluorophore, such that each transcription event results in a consequent increase in fluorescence, allowing for transcript production to be monitored in real time [208,

209]. Examining *fdxA* as the target gene, phosphorylation of purified DosR with PknH or PknD inhibited the ability of DosR to increase steady-state transcription (Fig 2.4A), corresponding with the decrease in binding to the *fdxA* promoter observed with PknH or PknD-phosphorylated DosR (Figs 2.3B, 4.6C and 4.6D).

dosR expression is itself upregulated by the very signals that the DosRS(T) system responds to [39, 77, 172]. We found that concentrations as low as 0.25 μM AcP-treated DosR resulted in an increase in target gene transcription rate, with maximal rates obtained at 0.5-1 μM DosR, before levels again decreased at concentrations ≥1.5 μM (Fig 2.4B, black dashed line). Interestingly, when purified DosR was phosphorylated by PknH or PknD, in addition to being treated with AcP, an increase in transcription rate was also observed, but with a narrower activation window, as the "de-activation" response occurred with a steeper decline (for example, 4.76 ± 1.67 AU/s and 6.10 ± 1.56 AU/s for 3 μM PknH and PknD-phosphorylated, AcP-treated DosR, respectively, versus 12.14 ± 1.26 AU/s for only AcP-treated DosR, $p < 0.01$ in each case; Fig 2.4B and 2.4C, compare blue and red dashed lines to black dashed line). Importantly, this de-activation response is dependent on the presence of DosR binding motifs ("DosR boxes") and not simply due to non-specific DNA coating, as no transcription decrease was observed for the ribosomal *rrnA*P3 promoter that is not controlled by DosR and lacks DosR boxes (Fig 2.4D). These biochemical results further demonstrate how STPK phosphorylation can alter DosR activity output, and also intriguingly show a concentration-dependent effect of AcP treatment (HK phosphotransfer) on DosR activity that is modulated by STPK phosphorylation. Together, these results illuminate how STPK phosphorylation of DosR

can affect its function, and suggests a mechanism by which the response of Mtb to key environmental signals can be tightly regulated.

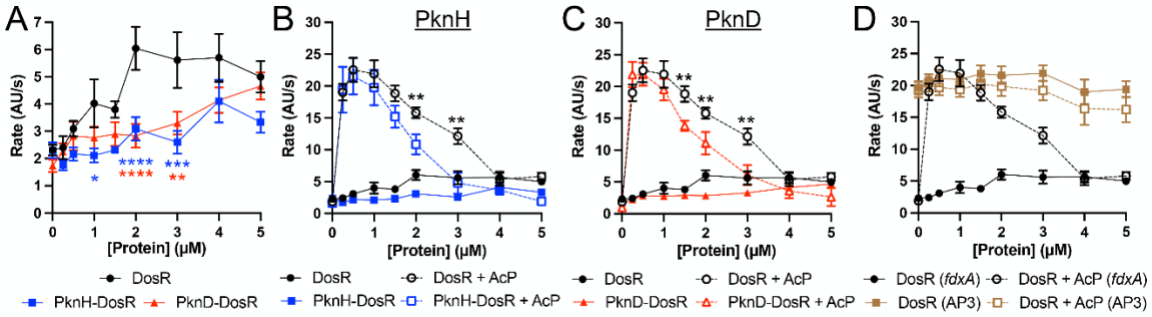

Figure 2.4. STPK phosphorylation of purified DosR decreases the level and alters concentration-dependence of steady-state transcription rates of its target genes. (A) STPK phosphorylation of DosR inhibits the ability of DosR to increase target gene steady-state transcription. A Spinach RNA aptamer assay was run with the *fdxA* promoter with different concentrations of indicated DosR protein. For "PknH-DosR" and "PknD-DosR", phosphorylation of DosR with PknH or PknD, respectively, was performed "on-bead" before final purification of the phosphorylated DosR utilized in the assay. Fluorescence (arbitrary units, "AU") was tracked over time on a plate reader, and steady-state rate calculated. Data are shown as means ± SEM from 3-8 experiments. p-values were obtained with a 2-way ANOVA with Tukey's multiple comparisons. p-value in blue and red correspond to those for PknH-DosR and PknD-DosR, respectively, as compared to DosR. * $p<0.05$, ** $p<0.01$, *** $p<0.001$, **** $p<0.0001$. (B and C) STPK phosphorylation alters the dynamics of activated DosR. A Spinach RNA aptamer assay was run with the *fdxA* promoter with different concentrations of indicated DosR protein, as in (A). (D) DosR concentration-dependent transcription is not observed with a promoter lacking DosR binding motifs. A Spinach RNA aptamer assay was run with the *fdxA* or *rrnA*P3 (no DosR binding motif) promoters with different concentrations of DosR protein, as in (A). 50 mM acetyl phosphate (AcP) was used where indicated. Data are shown as means ± SEM from 3-8 experiments. WT, PknH-DosR, and PknD-DosR data where shown in panels (B)-(D) are as shown in Fig 2.4A. The same DosR + AcP data set for the *fdxA* promoter is shown in panels (B)-(D). p-values were obtained with a 2-way ANOVA with Tukey's multiple comparisons. Significant p-values are shown for the PknH-DosR + AcP, or PknD-DosR + AcP, versus DosR + AcP proteins. ** $p<0.01$. The numerical data underlying the graphs shown in this figure are provided in Data File 4.1.

2.2.4 The STPK PknH regulates the DosR-dependent transcriptional response of Mtb to NO

Given our working hypothesis, supported by the observations above, that STPK activity is functionally relevant to regulation of the Mtb stress response, we finally sought to examine how a *pknH* deletion might alter the sensitivity of Mtb to NO. To this end, we first transformed WT, Δ*pknH*, and *pknH** (complemented mutant) with our NO/hypoxia-responsive *hspX'*::GFP reporter [59], and tested reporter response in different DETA NONOate concentrations. Markedly, *hspX'*::GFP reporter induction was higher at an intermediate DETA NONOate concentration (50 μM) with Δ*pknH* Mtb as compared to WT or *pknH** Mtb (Fig 2.5). In contrast, in the presence of 100 μM DETA NONOate, reporter induction was similar across all strains (Fig 2.5).

While the DosR regulon encompasses the subset of genes most highly induced upon Mtb exposure to NO, there is also a significant number of Mtb genes that are responsive to NO in a non-DosR-dependent manner [77, 143]. To more specifically probe

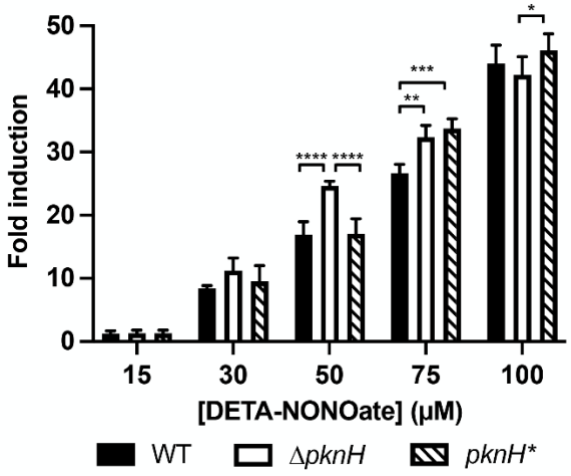

Figure 2.5. The STPK PknH regulates response of the *hspX'*::GFP reporter to NO. WT, Δ*pknH*, and *pknH** (complemented mutant) Mtb each carrying the *hspX'*::GFP reporter were exposed for 1 day to the indicated DETA NONOate concentrations, before fixation and reporter signal analysis via flow cytometry. Fold induction is in comparison to the untreated condition for each strain. Data are shown as means ± SEM from 3 experiments. p-values were obtained with a 2-way ANOVA with Tukey's multiple comparisons. Only significant comparisons are indicated. * $p<0.05$, ** $p<0.01$, *** $p<0.001$, **** $p<0.0001$. The numerical data underlying the graph shown in this figure are provided in Data File 1.

the relationship of PknH phosphorylation with DosR-mediated response of Mtb to NO, we thus next examined induction of DosR-dependent and -independent NO-responsive genes by qRT-PCR, examining induction across a range of DETA NONOate exposures as with the *hspX'*::GFP reporter assay. Analyses of three representative genes in the DosR regulon show markedly increased induction for all three genes in Δ*pknH* Mtb at the intermediate 50 μM DETA NONOate concentration that was restored to WT Mtb levels by complementation (Fig 2.6A), with induction levels at the higher 75 μM and 100 μM DETA NONOate concentrations similar across the strains (Fig 2.6B-6C), supporting the *hspX'*::GFP reporter data (Fig 2.5). Strikingly, no change in induction profile between WT and Δ*pknH* was observed at all DETA NONOate concentrations for the three NO-responsive, non-DosR-regulated genes tested (Fig 2.6D-2.6F).

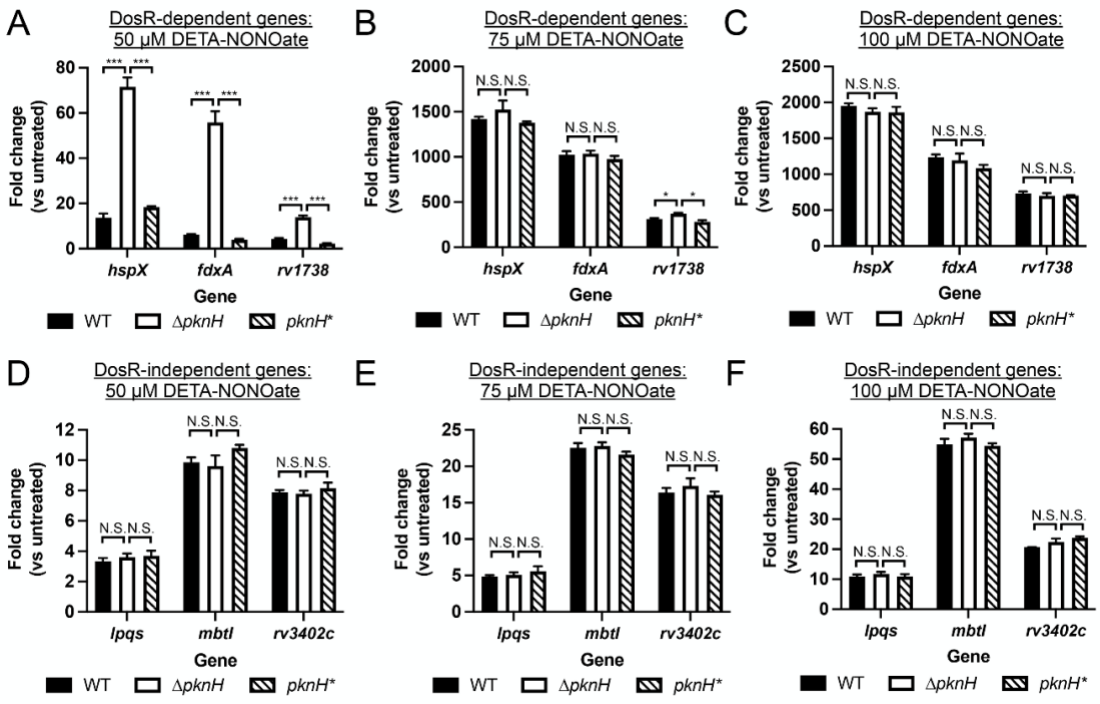

Figure 2.6. The STPK PknH regulates the DosR-dependent Transcriptional response of Mtb to NO. (A-C) Δ*pknH* Mtb exhibits increased induction of DosR-

dependent NO-responsive genes at intermediate DETA NONOate levels. Log-phase WT, Δ*pknH*, and *pknH** Mtb were exposed for 4 hours to 7H9, pH 7 media ± indicated DETA NONOate concentrations, before RNA was extracted for qRT-PCR analysis. (D-F) *pknH* deletion does not affect induction of DosR-independent NO-responsive genes. qRT-PCR analysis on DosR-independent NO-responsive genes were performed on samples obtained as in (A-C). In all cases, fold change compares each DETA NONOate condition to the control untreated condition for each strain. Data are shown as means ± SEM from 3 experiments, and p-values were obtained with unpaired t-tests with Holm-Sidak multiple comparisons. N.S. not significant, * $p<0.05$, *** $p<0.001$. The numerical data underlying the graphs shown in this figure are provided in Data File 4.1.

2.3 Discussion

The ability of Mtb to sense and respond to environmental cues is dependent on signal transduction regulatory mechanisms such as STPKs and TCSs, which are critical for bacterial adaptation and hence survival within a host [41, 131, 143, 178, 185, 186, 205, 210]. While the interplay between STPKs and TCSs has become increasingly appreciated, how such interplay may alter TCS function and thus the response of Mtb to environmental cues has remained understudied. Here, we uncover a role of STPK phosphorylation of TCSs as a fine-tuning regulatory mechanism that acts to provide an additional layer of regulation of TCS RR activity.

In particular, our findings that PknH phosphorylation of purified DosR decreases DNA binding affinity to target promoters and steady-state transcription of target genes, and that deletion of *pknH* in Mtb results in increased induction of DosR-dependent, but not DosR-independent, NO-responsive genes at intermediate levels of NO stress, strongly support that regulation of DosR by STPKs serve as a second axis of regulation, in addition to regulation by its cognate histidine kinases. A previous study had conversely reported increased binding of DosR to the *hspX* promoter when DosR and PknH were co-expressed in *Escherichia coli*, with DosR subsequently purified for EMSAs, as well as

decreased induction of several DosR regulon genes in Δ*pknH* Mtb upon NO exposure [170]. It is difficult, however, to separate out what other modifications may also occur in *E. coli*, and there were differences in the EMSA assays, with the previous study testing binding to separate DosR boxes present in the *hspX* promoter (38 bp or 54 bp segments), versus the longer DNA segments encompassing all DosR boxes upstream of the *hspX* promoter utilized in our study. Complementation was not shown for the Δ*pknH* transcriptional response phenotypes in that study [170], and differences in Mtb strain (H37Rv in the previous study versus CDC1551 here) and growth conditions between our studies may also account for the different results.

Notably, both the DosR T198 and T205 sites phosphorylated by PknH map within the α10 helix of the DosR crystal structure [211, 212]. DosR is thought to adopt two dimeric structures, one active and one inactive, that exist in equilibrium with each other as well as a monomeric form [213]. Phosphotransfer to the D54 site in the receiver domain favors the active, DNA-binding DosR, with the α10 helix from each monomer mediating the dimerization of that species, making this helix critical for protein activation [211, 213]. The T198 and T205 PknH phosphorylation sites are closely positioned in the DosR dimer interface in the DNA-binding conformation, and we thus posit that PknH phosphorylation of these sites shifts the equilibrium of DosR in such a way as to disfavor the active DNA binding-competent dimer form, resulting in the decreased DNA binding affinity and steady-state transcription observed. Examples of opposing effects of STPK and HK phosphorylation on activity of the corresponding RR have been previously reported in *S. aureus* and *Streptococcus agalactiae* [196, 197], and our data further

support this concept of STPKs serving to restrain TCS activity to ensure appropriate response.

Our attempt to generate a STPK phosphoablative DosR was unsuccessful, as mutation of the T198 and T025 sites to alanine residues resulted in a non-functional protein with poor DNA binding and minimal *fdxA* steady-state transcription (Fig 4.8). Interestingly, positioning of known or putative STPK phosphorylation sites close to or within the DNA binding region is also found for other Mtb TCS RRs such as MtrA and PhoP [150, 210, 214, 215], as well as in TCS RRs of other bacterial species [168, 193, 197]. In the case of the Mtb TCS RR PrrA, STPK phosphorylation occurs within the receiver domain, affecting Mtb response to various environmental signals [143]. Future studies seeking to uncover how STPK phosphorylation alters TCS structure and hence function will be important for continued insight into the role of STPKs as regulators of TCSs.

A key outstanding question is how STPK activity is regulated. Expression levels of STPKs have not generally been found to be affected by key environmental signals for Mtb, and Mtb encodes only a single Ser/Thr phosphatase, with broad activity across phosphorylated Ser/Thr residues [186]. The large number of targets for a given STPK would however strongly suggest a need for regulation of their activity, and indeed the basal activity level for many STPKs appears low, as evidenced by deletion mutants of the STPKs exhibiting little reduction in phosphosites, compared to WT Mtb, in standard rich media [150]. STPKs autophosphorylate and dimerization is required for their activation [186, 216, 217]; ligand triggering of such events thus represent a route for control of STPK activity separate from expression differences. Indeed in *B. subtilis*, the STPK PrkC

senses cell wall fragments, with binding of peptidoglycan fragments to its extracellular domain leading to phosphorylation and activation of an essential ribosomal GTPase involved in initiating vegetative growth [158]. In Mtb, a Δ*pknG* mutant is defective for growth when glutamate or asparagine is used as the sole nitrogen source, and phosphorylation of GarA, a key target of PknG, was greatest in the presence of these same amino acids, suggesting that these amino acids may act as triggers for PknG activity [218]. Intriguingly, we found almost complete overlap in the STPKs that interact with the PrrA and DosR RRs, both known to mediate Mtb response to NO and hypoxia [65, 66, 143]. A smaller subset of those same STPKs also interacted with PhoP, which like PrrA, functions as a global regulator of pH and Cl^- [59, 143]. Future studies analyzing the extent of phosphorylation of each RR by a given interacting STPK identified here, and testing whether the same environmental signals that drive TCS activity also affect STPK activity, will provide important insight into the coordination of TCS and STPK activity.

Finally, the RNA aptamer-based transcriptional assay utilized here provides a real time, quantitative, and high-throughput method with broad utility for understanding basal and regulated transcription dynamics. This encompasses the ability to test effects of different intrabacterial signals and regulatory factors on gene transcription kinetics, through to analysis of antibiotic-dependent inhibition of RNA polymerase on transcription steady-state rates [208, 209]. Interestingly, this transcriptional assay revealed a non-monotonic relationship between AcP-activated DosR concentration and target gene steady-state transcription rates. More specifically, after the expected increase in transcription with initial increases in DosR concentration, we observed an unexpected decrease in transcription with further DosR concentration increases, a phenomenon that

was dependent on the presence of DosR binding motifs on the target promoter. Strikingly, the slope of this "de-activation" was modulated by STPK phosphorylation. In *Mtb,* expression of the DosR regulon is markedly elevated upon initial exposure to NO or hypoxia [39, 77, 172], reflecting its role in mediating the early transcriptional response to these stresses. However, this induction is transient, and expression levels decline over time even in the continued presence of the inducing signal [78]. Our results suggest a possible negative feedback mechanism incorporating the DosR phosphorylation state, whereby active DosR concentrations above a threshold result in decreased target gene expression relative to the maximum activation at lower concentrations. The HK DosS has been reported to also possess phosphatase activity [219, 220]; defining how such phosphatase activity may work in concert with both the observed RR concentration dependence and STPK phosphorylation to enable a negative feedback loop in DosR regulon expression will be vital for understanding physiological adaptation of Mtb to environmental cues that are maintained over the course of a chronic infection.

TCSs and STPKs are the two major regulatory systems through which environmental signals are transduced into adaptive outputs in bacteria. Our findings here illustrate how STPK-mediated phosphorylation of TCS RRs can act to fine tune transcriptional outputs, serving to ensure response initiation only when appropriate. Our work establishes a framework for dissecting STPK-TCS interplay, and we propose that further studies probing the interactions of these two regulatory systems will continue to yield important insight into molecular pathways critical for Mtb environmental adaptation and host colonization.

2.4 Materials and Methods

2.4.1 Mycobacterial protein fragment complementation assays

Mycobacterial protein fragment complementation (M-PFC) assays were performed essentially as described previously [201]. The open reading frames of *dosR*, *prrA*, *phoP*, and *kdpE* were each cloned into pUAB100, generating C-terminal translational fusions to the murine dihydrofolate reductase (mDHFR) fragment F1,2 domain. All Mtb STPK genes were cloned into pUAB400, generating N-terminal translational fusions to the mDHFR fragment F3 domain. For STPKs with transmembrane domains (all except PknG and PknK), only the kinase domain was cloned. *M. smegmatis* transformed with each respective plasmid pair (each STPK with each RR) were plated on 7H11 plates supplemented with 25 µg/ml kanamycin and 50 µg/ml hygromycin, with TRIM added at 10, 20, 30, or 50 µg/ml. pUAB100 and pUAB400 plasmids containing the *Saccharomyces cerevisiae* GCN4 homodimerization domain served as the positive control [201]. As a negative control, *M. smegmatis* expressing the RR-mDHFR F1,2 fusion in pUAB100 with an empty pUAB400 plasmid was used. *M. smegmatis* transformants carrying mDHFR F3-PknB or mDHFR F3-PknI could not be obtained, and M-PFC assays with these STPKs were thus not pursued.

2.4.2 Recombinant protein expression and purification

The open reading frames of DosR and DosR-T198A/T205A were individually cloned into the isopropyl-β-D-1-thiogalactopyranoside (IPTG)-inducible pET-23a vector to generate a C-terminally 6xHis-tagged DosR and DosR-T198A/T205A, respectively. Expression constructs for the kinase domains of PknH and PknD were previously

described [217]. All constructs were transformed into *Escherichia coli* BL21(DE3) for recombinant expression and purification. For expression, 2 ml of overnight *E. coli* cultures started from single colonies were grown in 5 ml LB + 50 μg/ml ampicillin at 37°C and were used to inoculate 1 L LB media + 50 μg/ml ampicillin. Cultures were grown at 37°C, 160 rpm, until the culture reached an OD_{600} of ~0.6. Induction of constructs was initiated by adding 1 mM IPTG, and the cultures grown for an additional 16 hours at 16°C, 160 rpm. Afterwards, supernatants were removed, and pellets were stored at -80°C prior to further processing.

Recombinant purification of DosR and its variants and STPKs followed previously described protocols [60, 143]. The template for the DosR T198A/T205A mutant was generated using QuikChange mutagenesis of WT DosR (Agilent). To remove phosphorylated residues accrued from expression in *E. coli*, the protein was treated with alkaline phosphatase (Sigma #P0114) according to previously described protocols [221], when the protein was still bound to the nickel beads. Dephosphorylated DosR was then washed three times with a minimal low imidazole buffer (500 mM NaCl, 50 mM Tris, pH 7.5, 15 mM imidazole, 10% glycerol) to remove residual alkaline phosphatase. For *in vitro* phosphorylation of DosR, DosR still bound to nickel beads was treated with 1 μM PknH or PknD and incubated at room temperature in kinase buffer (40 mM Tris-HCl, pH 7.5, 2 mM $MnCl_2$, 20 mM $MgCl_2$, 2 mM DTT, 0.5 mg/mL BSA) for one hour. The nickel bead-bound DosR was then washed to remove the purified STPKs, prior to continuation of the protein purification protocol to obtain STPK-phosphorylated DosR. DosR protein was dialyzed into electrophoretic mobility shift assay (EMSA) buffer as described [199]. Protein concentrations were quantified by using a Bradford assay (Bio-Rad).

Mtb RNAP σ^A holoenzyme complex was purified by a 10X N-terminal His-tag on the alpha subunit, using pET-Duet-*rpoB-rpoC,* pAcYc-His*rpoA-rpoZ*, and pAC27-*sigA* plasmids, expressed and purified as previously described [209]. The final holoenzyme fractions were dialyzed into storage buffer (10 mM Tris-Cl, pH 7.0, 200 mM NaCl, 0.1 mM EDTA, 1 mM $MgCl_2$, 20 μM $ZnCl_2$, 2 mM DTT, 50% glycerol), concentrated to 4.5 μM (determined using an extinction coefficient of 280,425 M^{-1} cm^{-1}), aliquoted, flash frozen in liquid nitrogen, and stored at -80°C.

Mtb CarD and RbpA, in pET-SUMO plasmid vectors, were expressed, purified, and the His-SUMO tag removed as previously described [209, 222]. Eluted fractions were dialyzed overnight in 20 mM Tris, pH 8.0, 150 mM NaCl, 1 mM β-mercaptoethanol, then concentrated to 200 μM determined using extinction coefficients of 16,900 M^{-1} cm^{-1} for Mtb CarD and 13,980 M^{-1} cm^{-1} for Mtb RbpA.

2.4.3 Mass spectrometry

Protein samples underwent in-gel trypsin digestion at the Mass Spectrometry Technology Access Center at the McDonnell Genome Institute (MTAC@MGI) at Washington University School of Medicine. The resulting peptides were analyzed by LC-MS/MS using data-dependent acquisition on an Orbitrap Eclipse Tribad mass spectrometer (ThermoFisher Scientific). Data were searched against a custom *E. coli* BL21 (DE3) database supplemented with the DosR sequence, using Mascot software to identify phosphorylation on aspartic acid, serine, threonine, and tyrosine residues. In all samples, DosR accounted for at least 80% of the identified peptides and 99% sequence coverage of DosR was obtained.

2.4.4 Electrophoretic mobility shift assays

Electrophoretic mobility shift assays (EMSAs) were performed essentially as previously described [60, 223]. In brief, promoter regions for *hspX* (558 bp) and *fdxA* (221 bp) were amplified using IRDye 700 labeled primers (Integrated DNA technologies) and the PCR products purified using a QIAquick PCR purification kit (Qiagen). For acetyl phosphate-treated reactions, purified DosR-6xHis protein was treated as described previously [199]. Indicated amounts of unphosphorylated and phosphorylated DosR were mixed with 40 fmoles of DNA in EMSA buffer (25 mM Tris-HCl, pH 8, 20 mM KCl, 6 mM $MgCl_2$, 5% glycerol, 0.5 mM EDTA, 25 µg/ml salmon sperm DNA [199]) in a 10 µl final reaction volume. For competition EMSAs with unlabeled probes (*hspX*, *fdxA*, or the non-DosR target *rv2390c* [60]), 1 fmole of labeled probe was used, with indicated fold-molar excess ratios of unlabeled probe and protein in the reaction mixture. For all EMSAs, reactions were incubated at room temperature for 30 minutes and then run on non-denaturing 7.5% Tris-glycine gels in 0.5X Tris-borate-EDTA buffer at 4°C for ~4-4.5 hours. Gels were imaged using the 700 nm channel of an Odyssey CLx imaging system (LI-COR).

2.4.5 Fluorescence polarization assays

Fluorescence polarization (FP) experiments were performed using linear double-stranded DNA probes containing either the *hspX (85 bp) or fdxA (55 bp)* promoter labeled with Alexa Fluor 488 on the downstream 5' end (Integrated DNA Technologies). These were titrated with increasing concentrations of purified DosR, or PknH/PknD-treated DosR. 10 µl binding reactions in 384-well black, low volume, round bottom assay plates

(Corning) were sealed with optical adhesive film (Applied Biosystems) and measured on a CLARIOstar Plus plate reader (BMG LABTECH). DosR and its phosphorylation variants were serially diluted (1:1.5) from a 25 μM stock solution into binding buffer (25 mM Tris-HCl 8.0, 20 mM KCl, 6 mM $MgCl_2$, 10% glycerol), generating a final concentration range of 0-25 μM. Labeled DNA substrates were added to each well at a final concentration of 25 nM (5 μl of 50 nM stock). Plates were incubated at 37°C for 15 minutes before polarization measurements were taken using 485/520 nm excitation/emission FP filters.

For analysis, binding curves were fit to a Hill-type saturation equation using maximum likelihood estimation (MLE) implemented in R. Raw data were plotted, and fits were generated using the following Hill equation: $\Delta FP = (\Delta FP_{max} \cdot [P]^n)/ (K_d^n + [P]^n)$; Where ΔFP is the change in fluorescence polarization, [P] is the protein concentration (μM), ΔFP_{max} is the maximal signal, K_d is the apparent dissociation constant, and n is the Hill coefficient. For the DosR condition, where the data reach saturation, all three parameters were allowed to float. For the PknH-DosR and PknD-DosR conditions, which did not reach saturation, ΔFPmax was fixed to the value obtained from DosR alone, and MLE was used to estimate K_d and n, and the residual variance error parameter, σ. 95% confidence intervals (CIs) for parameter estimates were obtained by bootstrapping. For each condition, the Hill model was refit to 10000 synthetic datasets generated by data resampling. The 2.5^{th} and 97.5^{th} percentiles of the resulting distributions of parameter estimates defined the CI limits for each parameter. These confidence intervals were propagated to the fitted curves, producing shaded ribbons in the plots that visualize uncertainty in the predicted fluorescence polarization across the protein concentration

range. On the *hspX* promoter the residual variances (σ) were as follows: 16.3 ± 0.98 (DosR), 5.52 ± 0.47 (PknH-DosR), and 13.2 ± 0.91 (PknD-DosR). On the *fdxA* promoter, σ values were: 12.1 ± 0.89 (DosR), 12.9 ± 1.27 (PknH-DosR), and 10.0 ± 0.54 (PknD-DosR).

hspX probe:

/5Alex488N/ACAACAGGGTCAATGGTCCCCAAGTGGATCACCGACGGGCGC
GGACAAATGGCCCGCGCTTCGGGGACTTCTGTCCCTAGCCCTG

fdxA probe:

/5Alex488N/TGACGAATAAGGCCTTTGGTCCTTTCCGGTAGGGGTCTTTG
GATAGGCGCGATCC

2.4.6 RNA aptamer-based transcriptional assay

Aptamer-based transcription data was collected using a CLARIOstar Plus Microplate reader (BMG LABTECH) in a 384 well, low volume, round-bottom, non-binding polystyrene assay plate (Corning) with the corresponding Voyager analysis software and following a previously published protocol [209]. To measure multi-round, steady-state transcription kinetics in real-time, we monitored the change in 3,5-difluoro-4-hydroxybenzylidene imidazolinone (DFHBI) fluorescence upon binding to a transcribed, full-length RNA sequence containing the *fdxA* or *rrnA*P3 promoter [209] and the iSpinach D5 aptamer. All reactions were conducted at 37°C in 10 µl final volume in 20 mM Tris (pH 8.0 at 37°C), 40 mM NaCl, 75 mM potassium glutamate, 10 mM $MgCl_2$, 5 µM $ZnCl_2$, 20 µM EDTA, 5% glycerol with 1 mM DTT and 0.1 mg/ml BSA. Reactions

contained 100 nM RNAP holoenzyme, 20 μM DFHBI dye (Sigma Aldrich), 0.4 U/μl RiboLock RNase inhibitors (Thermo Scientific), CarD and RbpA at 1 μM and 2 μM, respectively, and dilutions of DosR from 1 μM to 50 μM. 2.5 μl stock rNTPs (Thermo Scientific) were injected *in situ* using the reader's automated reagent injector to a final concentration of 1 mM NTP. Data were acquired in 10-20 second intervals for up to 40 minutes total. A minimum of 3 technical replicates of the negative control (*i.e.*, no rNTPs) were collected and measured concurrently with the experimental data. Using the average of this negative control, the experimental data was corrected as previously described [208], bringing all starting fluorescence values to zero and correcting for any time-dependent drift in fluorescence. Between 2 and 8 independent experiments were collected for each condition with 3 technical replicates each. Standard deviations were used as a statistical weight during the linear regression analyses as previously described to obtain the steady-state rate [208].

2.4.7 Mtb strains and culture

Mtb CDC1551 was used as the parental strain for all assays here, and Mtb cultures were cultured and maintained as described previously, with 7H9 broth supplemented with 10% OADC, 0.2% glycerol, 0.05% Tween-80, and 100 mM MOPS used for buffering to pH 7.0 [224]. Generation of Δ*dosR*, Δ*pknH*, and their complements were constructed with methods as described previously [59]. The *dosR* deletion consisted of a region from the beginning of the open reading frame through nucleotide 650, while the *pknH* deletion encompassed the entire *pknH* open reading frame. Complementation in both cases utilized the respective endogenous promoters and open reading frames in the

integrating plasmid pMV306. The *hspX'*::GFP reporter introduced into indicated strains was previously reported [59]. Antibiotics were added as needed at the following concentrations: 100 μg/ml streptomycin, 50 μg/ml hygromycin, 50 μg/ml apramycin, and 25 μg/ml kanamycin.

2.4.8 qRT-PCR analyses

Mtb grown to log-phase (OD_{600} ~ 0.6) in aerated conditions was used to inoculate filter-capped T75 flasks laid flat, containing 12 ml 7H9, pH 7.0 ± indicated concentrations of DETA NONOate (Cayman Chemicals) at OD_{600} = 0.3. Bacteria were incubated for 4 hours, before RNA extracted as previously described [101]. qRT-PCR experiments were conducted and analyzed according to previously established protocols [225].

2.4.9 *hspX'*::GFP reporter assay

Indicated Mtb strains carrying the *hspX'*::GFP reporter were propagated to log phase (OD_{600} ~ 0.6) and subcultured to an OD_{600} = 0.05 in flat T75 flasks with filter caps containing 4 ml 7H9, pH 7. After 4 passages, Mtb was subcultured at OD_{600} = 0.05 in 7H9, pH 7.0 media with 0, 15, 30, 75, or 100 μM DETA NONOate. 1-day post-exposure, culture aliquots were taken and fixed in 4% paraformaldehyde. Reporter signal was analyzed via flow cytometry as previously described [225].

2.4.10 Statistical analyses

GraphPad Prism software was used for all statistical analyses, with $p < 0.05$ considered significant. The statistical test used for a given assay is described in the figure legends.

2.5 Attribution of work

NRS and ST conceived and designed the study. The M-PFC assays were conducted by NRS and AMVE, with assistance from Elizabeth Billings and Jannessa Ya for the KdpE experiments. Fluorescence polarization and RNA aptamer-based transcriptional assays were performed by ARM. The CDC1551 Δ*pknH* Mtb strain was originally generated by Calvin Johnson. All other experiments were performed by NRS. NRS and ST wrote the original draft of the manuscript, and NRS, ARM, EAG, and ST edited the manuscript.

Chapter 3: Discussion

3.1: Overview

My thesis establishes a framework for signal transduction in Mtb in which STPKs act alongside canonical TCS pathways to shape transcriptional responses in the context of host infection. Central to this model is the concept that STPK phosphorylation constitutes a second regulatory axis that can modulate RR activity in a manner that is more nuanced rather than simply reinforcing or duplicating HK signaling. Using DosR as a primary example, my work demonstrates that STPK phosphorylation influences DNA binding, transcription kinetics, and sensitivity to environmental stimuli, thereby refining the bacterium's response to NO and hypoxic stress. Extending beyond DosR, interaction and functional data for additional regulators, including PhoP and KdpE, support that this layered regulatory mechanism is broadly applicable across multiple TCSs, positioning STPKs as integrators of cellular physiology with environmental sensing pathways.

Several questions emerge from this work regarding how STPK phosphorylation shapes transcriptional regulation at a structural level. My findings with DosR suggest that phosphorylation within specific helices of the protein can influence dimer stability and conformational equilibria, thereby modulating transcriptional activation. The observation that similar phosphorylation sites occur near functional domains in other RRs raises the possibility of a conserved mechanism, however, this question remains to be answered. A key next step to address this question will be to define how phosphorylation alters RR-DNA interactions and oligomerization in real time. Such studies will be critical for understanding how post-translational signaling integrates with transcriptional control in Mtb.

The findings presented here also raise important questions about how STPK activity itself is regulated and how this additional layer of control contributes to bacterial adaptation during host infection. Understanding when and where phosphorylation occurs, the extent to which RRs are modified under different environmental conditions, and how kinase activation correlates with HK signaling will be critical next steps. Quantitative phosphoproteomic approaches, single-cell transcriptional analyses, and *in vivo* infection models will provide valuable insight into how these signaling systems support successful Mtb host infection. Further, these questions prompt a broader reconsideration of how regulatory flexibility is achieved in Mtb throughout host infection. My findings raise the possibility that STPK-mediated regulation can be dynamic, relying on context-dependent tuning of gene expression, and offer a conceptual framework for how the bacterium copes with changing host environments. Several questions remain to be answered, particularly regarding how these phosphorylation events are temporally coordinated, how they intersect with other signaling pathways, and whether similar regulatory logic applies across infection niches. Exploring these areas represents an important direction for future research into Mtb signal integration and persistence.

3.2: Importance of STPK phosphorylation site on TCS RR structure and function

The findings in my thesis point toward structural positioning as a critical determinant of how STPK phosphorylation shapes RR behavior. In particular, a significant implication of my work is that STPK modification can bias equilibria among functionally distinct structural states rather than simply switching RRs “on” or “off”. Understanding this at a mechanistic level will require moving beyond functional readouts

toward direct structural and biophysical studies. DosR is a tractable model for pursuing these questions given its crystal structure is already known, and in chapter 2 of this thesis, we provide evidence that phosphorylation, occurring near the α10 helix of DosR (Fig 3.1A), influences dimer stability and transcriptional competence (Fig 3.1B). Biochemical measurements presented in Chapter 2 of this thesis further support this interpretation. In particular, fluorescence polarization experiments demonstrated that phosphorylation of DosR by the STPKs PknH or PknD reduced binding affinity to the promoters of the target genes *hspX* and *fdxA* (Fig 2.3 and Fig 4.6), indicating that phosphorylation perturbs the formation or stability of transcriptionally competent DosR-DNA complexes. Consistent with this observation, *in vitro* transcription assays revealed that STPK phosphorylation decreases steady-state transcription from DosR target promoters while also altering the concentration dependence of transcriptional activation (Fig 2.4).

Among key outstanding questions, it remains unclear if STPK phosphorylation shifts DosR toward a monomeric versus a dimeric state, or if it alters the stability or lifetime of active dimers. Future experiments to directly test these possibilities could include analytical ultracentrifugation or size exclusion chromatography-multi-angle laser light scattering (SEC-MALLS) [226, 227]. These techniques would produce a quantitative measurement of DosR oligomeric equilibria. Importantly, such approaches would establish whether STPK regulation acts at the level of dimerization itself, modulating the respective proportions of protein species. Complementary hydrogen-deuterium exchange mass spectrometry (HDX-MS) would map phosphorylation-induced changes in protein dynamics and solvent accessibility [228], revealing whether phosphorylation destabilizes the α10 interface or propagates allosteric effects to DNA-

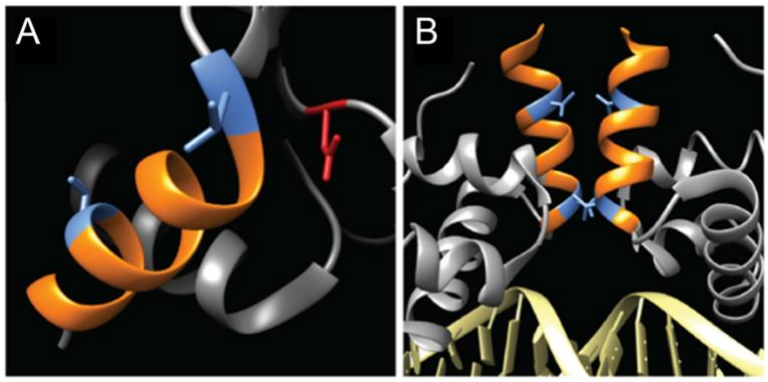

Figure 3.1. Phosphorylated residues of interest on DosR. Threonine 198 and 205 (PknH targets) are shown in blue and helix 10 in orange. (A) Free DosR structure (PDB:3C3W): Aspartic acid 54 (HK phosphotransfer target) is shown in red. (B) DosR dimer bound to DNA (PDB:1ZLK). Note, T198 and T205 on helix 10 of each monomer are closely positioned in the DosR dimer interface in the DNA binding conformation.

binding regions [211, 213]. In parallel, understanding if phosphorylation affects exchange kinetics between active and inactive DosR protein conformations is critical. To test this, single-molecule FRET provides an additional layer of resolution by enabling observation of conformational transitions in real time, thereby distinguishing whether phosphorylation primarily alters equilibrium populations or instead modulates the kinetics of interconversion between states [229].

An important conceptual challenge emerging from my thesis work is the need to separate structural perturbation from regulatory phosphorylation. As described in chapter 2, introduction of phosphoablative (T→A) mutations at STPK phosphorylation sites in DosR showed that this single residue substitution itself disrupted protein function, precluding its use for the directed study of STPK phosphorylation effects. In chapter 2 we also show through M-PFC protein-protein interaction mapping that PhoP and KdpE, like DosR, physically associate with multiple STPKs, displaying both overlap and specificity in their interaction profiles (Fig 2.1). Therefore, we hypothesized that these RRs are also

subject to regulation by STPKs. Using published global phosphoproteomic data [150], we generated mutations at sites predicted to be phosphorylated by STPKs in both RRs, PhoP (T177A/T235A) and KdpE (T100A). However, introduction of these mutations in PhoP resulted in a profound defect in transcriptional induction of Mtb in response to acidic pH and high [Cl^-], closely phenocopying a Δ*phoP* Mtb mutant rather than the wild type or complemented mutant (Fig 3.2A). This loss of inducible transcription is accompanied by

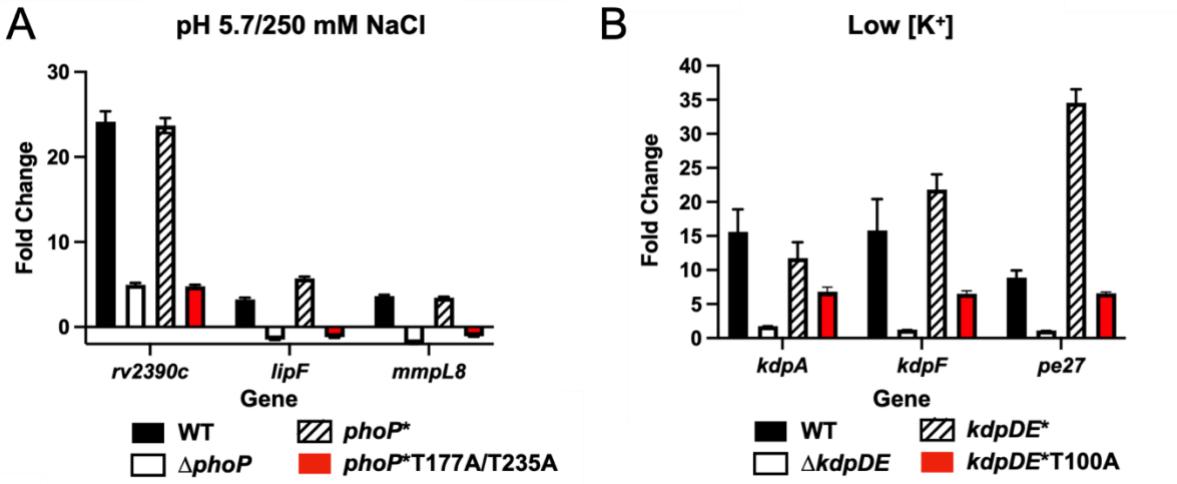

Figure 3.2. Preservation of STPK phosphorylation sites on TCS RRs is critical for transcriptional response to environmental signals. (A) Preservation of STPK phosphorylation sites on the RR PhoP is critical for induction of acidic pH regulon genes. Log-phase WT, Δ*phoP*, *phoP** (complemented mutant), and *phoP**T177A/T235A Mtb were exposed for 4 hours to 7H9, pH 5.7 + 250 mM NaCl before RNA was extracted for qRT-PCR. Fold change compares the pH 5.7 + 250 mM NaCl condition to the control untreated condition. *rv2390c*, is in both the pH and Cl^- regulons. *lipF* and *mmpL8* are members of the pH but not the Cl^- regulon. (B) Preservation of STPK phosphorylation sites on the RR KdpE is critical for induction of KdpDE regulon genes in response to low [K^+]. Log-phase WT, Δ*kdpDE*, *kdpDE** (complemented mutant), and *kdpDE**T100A Mtb were exposed for 4 hours to 7H9, pH 7 + low [K^+] before RNA was extracted for qRT-PCR. Fold change compares the low [K^+] condition to the control untreated condition. *sigA* was used as the control gene, and data are shown as means ± SEM from 3 experiments except for (B), which is a single experiment and shown as means ± SD. p-values were obtained with an unpaired t-test. *** $p<0.001$, **** $p<0.0001$.

a striking growth consequence in Mtb similar to Δ*phoP* Mtb, with growth not slowed in the presence of acidic pH [96] (Fig 3.3A). A comparable, though distinct, effect is observed when the KdpE T100A mutant is exposed to K^+-limiting conditions. Namely, upon introduction of this mutation into Mtb, we observed a significantly reduced induction of KdpE-regulated genes by qRT-PCR (Fig 3.2B), and this was translated into a measurable growth phenotype in Mtb (Fig 3.3B). As with the DosR-TI198A/T025A mutation, it is however difficult to directly ascribe these phenotypes to loss of STPK phosphorylation, versus functional defects arising from mutation of the site itself. One promising strategy to address this challenge is the use of genetic code expansion to incorporate phospho-amino acids site-specifically into the RRs [230]. This approach enables direct installation of phospho-serine or phospho-threonine at defined positions without altering the

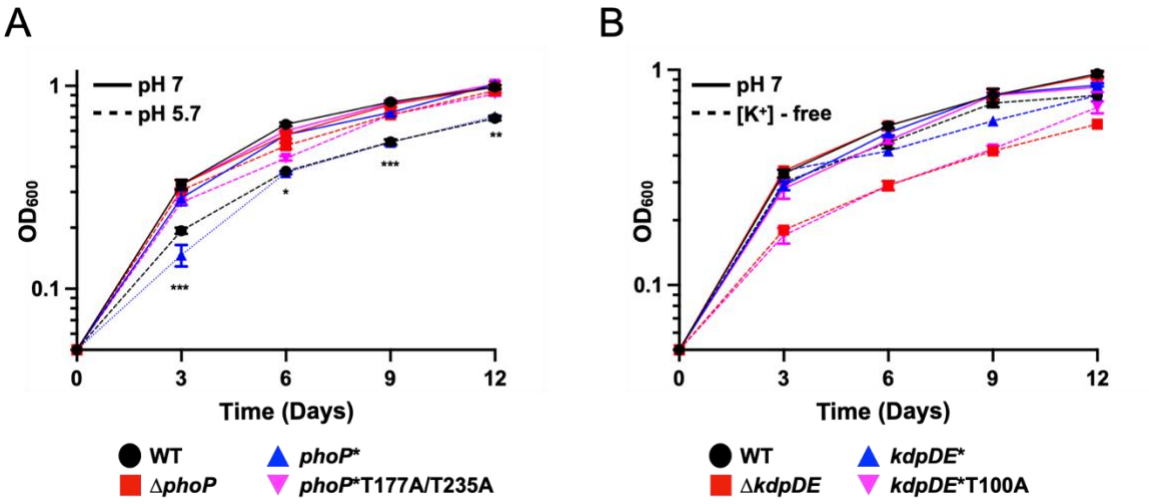

Figure 3.3. Preservation of STPK phosphorylation sites on TCS RRs is important for Mtb growth control in response to environmental signals. (A) STPK phosphorylation of PhoP alters Mtb growth control in acidic conditions. WT, Δ*phoP*, *phoP** (complemented mutant), and *phoP**T177A/T235A Mtb were grown in 7H9, pH 7 or pH 5.7 media and OD_{600} tracked over time. Data are shown as means ± SEM from 3 experiments. p-values were obtained with an unpaired t-test comparing *phoP**177A/235A against *phoP** in the 7H9, pH 5.7 media condition. * $p<0.05$, ** $p<0.01$, *** $p<0.0001$. (B) A STPK phosphoablative *kdpDE**T100A mutant is attenuated for growth in limiting [K_+]. WT, Δ*kdpDE*, *kdpDE** (complemented mutant), and *kdpDE**T100A Mtb cultures were grown in 7H9, pH 7 or K_+-free 7H9 and OD_{600} tracked over time. Data are shown as means ± SEM from 2 experiments.

surrounding side-chain chemistry, thereby avoiding the structural perturbations introduced by alanine substitution and should therefore permit robust interrogation of the true effects of phosphorylation/non-phosphorylation at these sites [230]. Applying this strategy to DosR, PhoP, or KdpE would allow direct comparison of phosphorylated and unmodified states in biochemical assays of DNA binding, oligomerization, and transcriptional activation.

Linking the structural effects of DosR phosphorylation to genome-wide regulatory behavior represents another critical next step. If phosphorylation subtly alters DNA-binding affinity or cooperativity, its impact may appear as changes in which promoters are preferentially occupied rather than simple activation or repression. ChIP-seq comparing phosphorylated and non-phosphorylated states could test whether phosphorylation redistributes RR occupancy across the genome [231]. Coupling this approach with transcriptomics under graded stimuli would test whether phosphorylation shifts activation thresholds or narrows dynamic ranges [232]. These experiments would directly probe whether structural modulation translates into quantitative regulatory tuning at a broader level.

Finally, a broader conceptual question raised by my thesis work is if STPKs exploit structural “pressure points” in RRs as a general regulatory principle. If so, phosphorylation may function as a rheostat that functions to subtly adjust regulatory sensitivity. My work raises the possibility that STPKs target structurally strategic positions precisely because small perturbations at these sites can yield strong regulatory consequences. Determining whether this represents an evolved design principle in Mtb signaling is an exciting avenue for future research.

3.3: Regulation of STPK activity

An important, unresolved question related to this work is how STPK activity is regulated in Mtb and under what physiological conditions RR phosphorylation occurs *in vivo*. While my thesis establishes that STPK-dependent phosphorylation can modulate RR function, the upstream signals and constraints that govern kinase activation remain unclear. Mtb encodes 12 STPKs but only a single annotated Ser/Thr phosphastase, PstP [233, 234], implying that kinase activity must be tightly controlled to prevent indiscriminate phosphorylation.

Focusing on DosR, we observed that loss of PknH selectively altered transcriptional responses under specific inducing conditions. This result suggests that STPK functions to fine-tune, rather than overwrite, canonical TCS signaling. In this context, baseline STPK phosphorylation levels might be expected to be low, or short-lived, and their regulatory impact would depend on timing relative to HK-mediated activation. To test this model would require direct measurement of phosphorylation stoichiometry and kinetics under relevant, defined environmental conditions. Future studies should prioritize quantitative approaches that assess both STPK phosphorylation site occupancy and temporal dynamics of RR phosphorylation. Targeted mass spectrometry with isotope-labeled standards, combined with time-resolved phosphoproteomics, would allow for determination of whether phosphorylation correlates with entry into or recovery from specific stress responses such as NO [235, 236]. Such experiments could distinguish between phosphorylation as a trigger for RR state transitions versus a mechanism for modulating the amplitude of the response. In parallel, measuring kinase autophosphorylation may also be informative, as most Mtb STPKs

require autophosphorylation for full catalytic activity [186]. Defining when and how these kinases become activated will be essential for understanding their contribution to RR regulation.

Another question that warrants further investigation is how STPKs are spatially regulated. Some STPKs can localize to the cell envelope, septum, or poles, suggesting that substrate accessibility may be restricted by subcellular organization [156, 217]. If RR phosphorylation depends on colocalization with active kinases, this would provide a mechanism for selective modification without broad disruption of transcriptional programs. Future experiments that combine localization studies with phosphosite quantification would therefore help determine whether spatial proximity serves as a factor in STPK-RR signaling.

Finally, it remains unclear whether the signals that activate STPKs overlap with those sensed by TCS pathways and/or are distinct. For example, DosR responds primarily to NO and hypoxia, whereas STPKs such as PknH have been linked to cell envelope and metabolic stress [161, 163]. This raises the possibility that STPKs provide a secondary layer of regulation that integrates orthogonal signals rather than duplicating inputs integrated by TCSs. Addressing this question will require systematic comparison of kinase activation and RR phosphorylation across diverse host-relevant conditions, including within macrophages and animal infection models. Such studies will be necessary to place STPK activity within the broader framework of environmental signal integration in Mtb.

Taken together, these considerations highlight that a complete understanding of RR activity depends on defining not just HK activity, but when partner STPKs are active,

how their activity is constrained, and how phosphorylation states change during infection. Clarifying these points represents an important next step toward a mechanistic model of layered phosphorylation-dependent regulation in Mtb.

3.4: Role of STPK-mediated regulation throughout host infection

The findings in this thesis support that STPK-mediated phosphorylation contributes to how Mtb modulates transcriptional responses during infection. Host environments are not static, and the bacterium experiences fluctuating combinations of NO, hypoxia, redox stress, and nutrient limitation across intracellular and extracellular niches in the host [36, 39, 59, 60, 77]. Under these conditions, sustained maximal activation of stress regulons is unlikely to be uniformly beneficial. Therefore, a regulatory system that permits graded or reversible control would therefore provide an advantage as bacteria transition between microenvironments. STPK-dependent modification of RRs is consistent with such a need.

The results presented in Chapter 2 of this thesis demonstrate that STPK signaling contributes directly to Mtb response and regulation of NO. Using an *hspX*'::GFP transcriptional reporter, deletion of the STPK *pknH* altered the magnitude of DosR-dependent transcriptional activation during NO exposure (Fig 2.5). Consistent with this reporter phenotype, transcriptional analyses revealed that expression of multiple DosR-regulated genes was altered in the Δ*pknH* Mtb mutant following NO treatment (Fig 2.6). These data indicate that STPK signaling influences the transcriptional output of the DosR regulon under nitrosative stress conditions, like those encountered during infection. Further, in this context, PknH can function as a molecular "brake" on DosR activity,

restraining premature activation of the dormancy response until the bacterium experiences a sufficiently strong environmental signal. In this model, phosphorylation of DosR by PknH would bias the protein toward a less transcriptionally active state, thereby preventing inappropriate activation of the DosR regulon under conditions in which entry into dormancy would be unnecessary or energetically costly. Such a regulatory mechanism would ensure that the dormancy program is deployed only when environmental conditions truly warrant the metabolic transition associated with persistence. In the absence of PknH, this regulatory brake is removed, allowing DosR-dependent transcription to become more readily activated at intermediate NO concentrations, as observed in the reporter assays (Fig 2.5) and transcriptional analyses of DosR-regulated genes (Fig 2.6) described in Chapter 2.

During infection, bacteria residing within host tissues are unlikely to experience uniform exposure to NO. Instead, macrophage-derived NO is generated locally and is expected to form spatial gradients within infected cells and granulomatous lesions. Consequently, individual bacteria may encounter distinct levels of nitrosative stress depending on their precise location within host tissue. Within this spatially heterogeneous environment, NO concentrations could act as positional cues that inform the bacterium of its proximity to activated immune cells. In this framework, the concentration range that produces maximal DosR activation *in vitro* may correspond to physiologically relevant signaling experienced by bacteria residing within or beside activated macrophages or other immune microenvironments. STPK-mediated modulation of DosR activity may therefore enable Mtb to interpret these gradients of host-derived NO. By acting as a molecular brake, PknH could prevent premature activation of the dormancy program

when NO levels are low, while still allowing robust activation once a threshold of immune pressure is reached. This mechanism would allow the bacterium to generate a graded transcriptional response that reflects its position within the host environment.

How this regulation manifests throughout the course of host infection remains unclear. One unresolved question is whether STPK-mediated tuning primarily affects the timing of regulon engagement, the reversibility of activation, or the stability of transcriptional states once induced. Addressing this will require approaches that capture regulatory behavior across infection stages rather than under static conditions. Reporter systems that track DosR-dependent transcription over time in infected cells could clarify whether STPK signaling influences entry into, maintenance of, or exit from DosR-mediated dormancy-associated states [59, 174].

Finally, it remains to be established how broadly this regulatory mechanism extends beyond DosR to other RRs. Other RRs important in host adaptation, including PhoP and KdpE, contain candidate STPK phosphosites [150], suggesting that layered regulation is not unique to DosR. Determining whether similar modulatory relationships operate across pathways will be necessary to define whether STPK-dependent tuning is a specialized mechanism or a general principle of environmental response in Mtb.

Together, these considerations point toward a model in which STPK-mediated phosphorylation contributes to regulatory flexibility during infection by modulating the range and persistence of RR activity. Clarifying how this tuning operates *in vivo* represents an important next step in understanding how Mtb maintains physiological adaptability within heterogeneous host environments.

3.5: Conclusion

This thesis work builds on a model in which STPKs function as a second regulatory axis in Mtb signal transduction that operates alongside canonical TCS pathways. By integrating biochemical, structural, and functional analyses, this work demonstrated that STPK phosphorylation modulates RR activity, influencing DNA binding, oligomerization, and gene expression in ways that enable graded and context-dependent adaptation to host-derived stresses. Extension of this framework towards additional RRs linked to Mtb virulence, such as PhoP, or other signal response pathways, such as KdpE, will be critical for understanding how this layered regulatory strategy applies across Mtb TCSs. Moving forward, examining real-time dynamics of RR phosphorylation, resolving the structural consequences of these modifications, and determining how environmental cues that activate TCSs influence STPK activity will be a priority. Addressing these questions will be essential for developing predictive models of signal integration and for fully understanding how intersecting phosphorylation networks support long-term bacterial survival during infection.

Chapter 4: Appendix

Sontag NR, Ruiz Manzano A, Ecker AMV, Galburt EA, Tan S. (2026) Serine/threonine protein kinase phosphorylation of DosR alters target gene transcription mechanics and regulates *Mycobacterium tuberculosis* response to nitric oxide stress. PLoS Genetics 22(2): e1012043. doi: 10.1371/journal.pgen.1012043.

4.1: Chapter 2 Supplemental Information

4.1.1: Chapter 2 Supplemental Figures

STPK \ RR	DosR	PrrA	PhoP	KdpE
PknA	No	No	No	No
PknD	Yes	Yes	No	No
PknE	Yes	Yes	Yes	Weaker (up to 30 µg/ml TRIM)
PknF	Yes	Yes	Yes	Weaker (up to 30 µg/mL TRIM)
PknG	Yes	No	No	No
PknH	Yes	Yes	Yes	No
PknJ	Weaker (up to 30 µg/ml TRIM)	Yes	No	No
PknK	No	No	No	No
PknL	No	No	No	No

Figure 4.1. There is both overlap and specificity in interactions between STPKs and TCS RRs. Summary table of interactions between the RRs PrrA, DosR, PhoP, and KdpE with various STPKs (kinase domains only for all except PknG and PknK) as determined by M-PFC assays. Results are representative of 2-3 independent experiments.

A

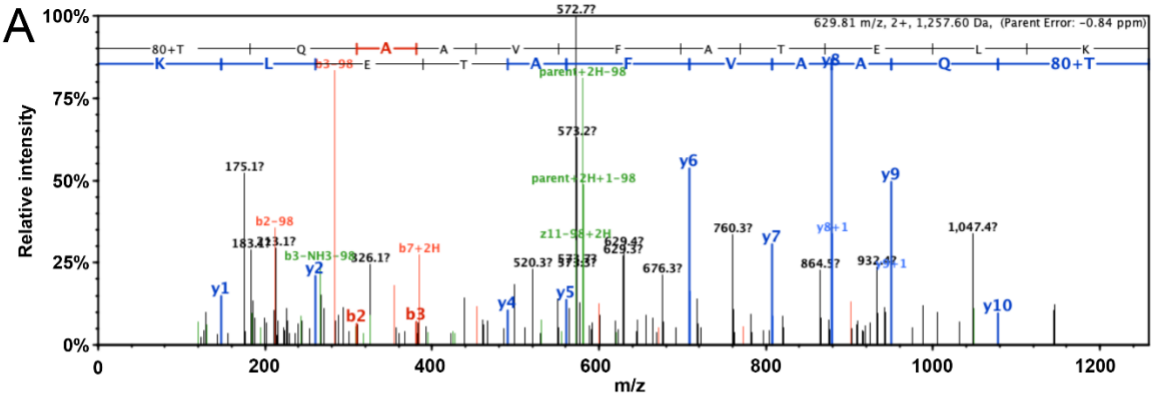

B

B	B Ions (m/z)	B+2H	B-NH_3	B-H_2O	AA	Y Ions (m/z)	Y+2H	Y-NH_3	Y-H_2O	Y
1	182.02			164.01	T+80	1,258.61	629.81	1,241.58	1,240.60	11
2	310.08		293.05	292.07	Q	1,077.59	539.3	1,060.57	1,059.58	10
3	381.12		364.09	363.11	A	949.54	475.27	932.51	931.52	9
4	452.15		435.13	434.14	A	878.5	439.75	861.47	860.49	8
5	551.22		534.2	533.21	V	807.46	404.23	790.43	789.45	7
6	698.29	349.65	681.26	680.28	F	708.39	354.7	691.37	690.38	6
7	769.33	385.17	752.3	751.32	A	561.32		544.3	543.31	5
8	870.38	435.69	853.35	852.37	T	490.29		473.26	472.28	4
9	999.42	500.21	982.39	981.41	E	389.24		372.21	371.23	3
10	1,112.50	556.75	1,095.48	1,094.49	L	260.2		243.17		2
11	1,258.61	629.81	1,241.58	1,240.60	K	147.11		130.09		1

Figure 4.2. Annotated MS/MS spectrum confirming phosphorylation of DosR T198 after PknH treatment. (A) MS/MS spectrum of the peptide tQAAVFATELK (m/z 629.81, z = 2). Observed *b* and *y* ions, along with neutral-loss fragments (-98 Da), are indicated. (B) Fragmentation map displaying detected ions (red = b; blue = y; green = neutral-loss/derived fragments) confirming site localization at T198. Spectra were searched using Mascot v2.8.3 and MSFragger in Scaffold 5.3.3 (precursor tolerance = 10 ppm; fragment tolerance = 0.05 Da; fixed Cys +57.02; variable phospho +79.97 [STY]; enzyme = trypsin, ≤3 missed cleavages; peptide/protein FDR < 1%; peptide probability > 90%).

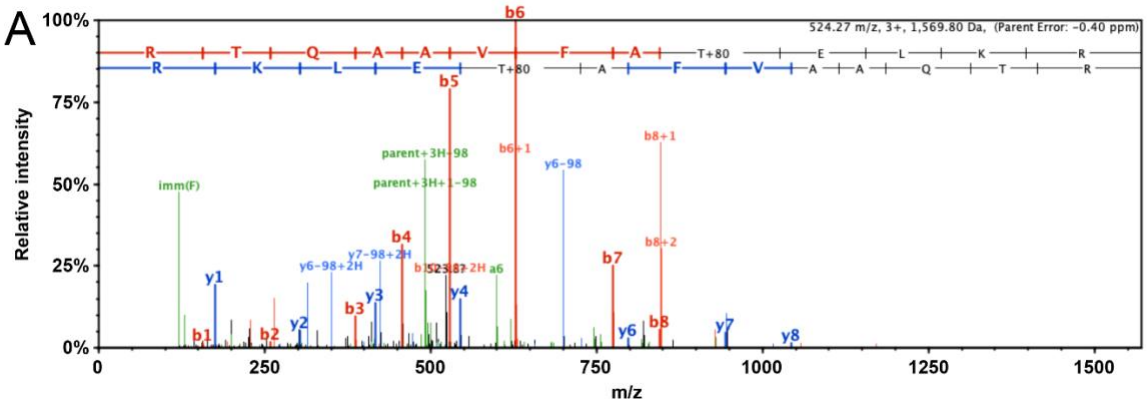

B

B	B Ions (m/z)	B+2H	B-NH_3	B-H_2O	AA	Y Ions (m/z)	Y+2H	Y-NH_3	Y-H_2O	Y
1	157.11	79.06	140.08		R	1,570.81	785.91	1,553.78	1,552.80	13
2	258.16	129.58	241.13	240.15	T	1,414.71	707.86	1,397.68	1,396.70	12
3	386.21	193.61	369.19	368.2	Q	1,313.66	657.33	1,296.64	1,295.65	11
4	457.25	229.13	440.23	439.24	A	1,185.60	593.31	1,168.58	1,167.59	10
5	528.29	264.65	511.26	510.28	A	1,114.57	557.79	1,097.54	1,096.56	9
6	627.36	314.18	610.33	609.35	V	1,043.53	522.27	1,026.50	1,025.52	8
7	774.43	387.72	757.4	756.42	F	944.46	472.73	927.43	926.45	7
8	845.46	423.24	828.44	827.45	A	797.39	399.2	780.37	779.38	6
9	1,026.48	513.74	1,009.45	1,008.47	T+80	726.35	363.68	709.33	708.34	5
10	1,155.52	578.26	1,138.49	1,137.51	E	545.34	273.17	528.31	527.33	4
11	1,268.60	634.81	1,251.58	1,250.59	L	416.3	208.65	399.27		3
12	1,396.70	698.85	1,379.67	1,378.69	K	303.21	152.11	286.19		2
13	1,570.81	785.91	1,553.78	1,552.80	R	175.12	88.06	158.09		1

Figure 4.3. Annotated MS/MS spectrum confirming phosphorylation of DosR T205 after PknH treatment. (A) MS/MS spectrum of the peptide RTQAAVFAtELKR (m/z 524.27, z=3). Observed *b* and *y* ions, along with neutral-loss fragments (-98 Da), are indicated. (B) Fragmentation map displaying detected ions (red = b; blue = y; green = neutral-loss/derived fragments) confirming site localization at T205.

A

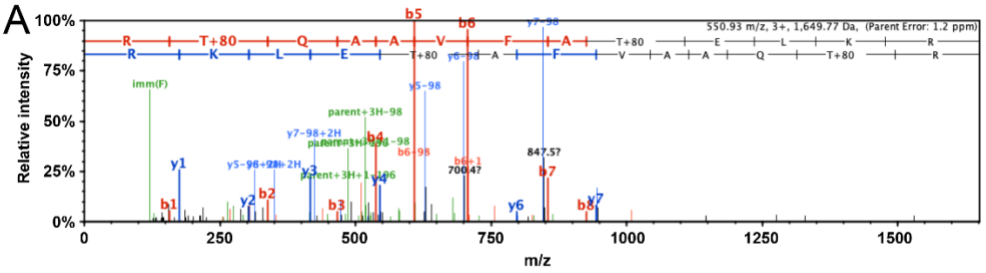

B

B	B Ions (m/z)	B+2H	B-NH_3	B-H_2O	AA	Y Ions (m/z)	Y+2H	Y-NH_3	Y-H_2O	Y
1	157.11	79.06	140.08		R	1,650.78	825.89	1,633.75	1,632.77	13
2	338.12	169.56	321.1	320.11	T+80	1,494.68	747.84	1,477.65	1,476.66	12
3	466.18	233.59	449.15	448.17	Q	1,313.66	657.33	1,296.64	1,295.65	11
4	537.22	269.11	520.19	519.21	A	1,185.60	593.31	1,168.58	1,167.59	10
5	608.26	304.63	591.23	590.24	A	1,114.57	557.79	1,097.54	1,096.56	9
6	707.32	354.17	690.3	689.31	V	1,043.53	522.27	1,026.50	1,025.52	8
7	854.39	427.7	837.37	836.38	F	944.46	472.73	927.43	926.45	7
8	925.43	463.22	908.4	907.42	A	797.39	399.2	780.37	779.38	6
9	1,106.44	553.73	1,089.42	1,088.43	T+80	726.35	363.68	709.33	708.34	5
10	1,235.49	618.25	1,218.46	1,217.48	E	545.34	273.17	528.31	527.33	4
11	1,348.57	674.79	1,331.54	1,330.56	L	416.3	208.65	399.27		3
12	1,476.66	738.84	1,459.64	1,458.65	K	303.21	152.11	286.19		2
13	1,650.78	825.89	1,633.75	1,632.77	R	175.12	88.06	158.09		1

Figure 4.4. Annotated MS/MS spectrum confirming phosphorylation of DosR T198 and T205 after PknH treatment. (A) MS/MS spectrum of the peptide RtQAAVFAtELKR (m/z 550.93, z=3). Observed *b* and *y* ions, along with neutral-loss fragments (-98 Da), are indicated. (B) Fragmentation map displaying detected ions (red = b; blue = y; green = neutral-loss/derived fragments) confirming site localization at T198 and T205.

A

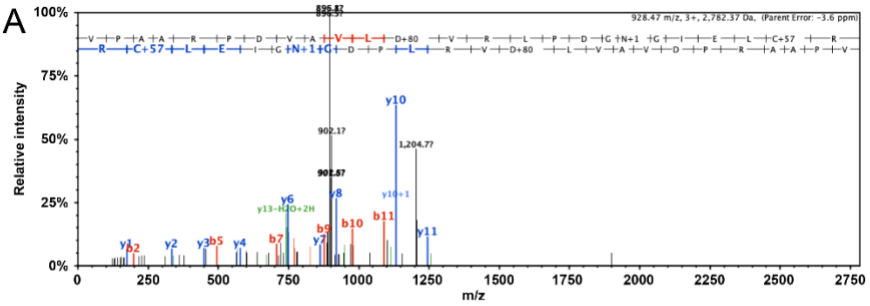

B

B	B Ions (m/z)	B+2H	B-NH_3	B-H_2O	AA	Y Ions (m/z)	Y+2H	Y-NH_3	Y-H_2O	Y
1	100.08	50.54			V	2,783.39	1,392.20	2,766.36	2,765.38	25
2	197.13	99.07			P	2,684.32	1,342.67	2,667.30	2,666.31	24
3	268.17	134.59			A	2,587.27	1,294.14	2,570.24	2,569.26	23
4	339.2	170.1			A	2,516.23	1,258.62	2,499.21	2,498.22	22
5	495.3	248.16	478.28		R	2,445.20	1,223.10	2,428.17	2,427.19	21
6	592.36	296.68	575.33		P	2,289.09	1,145.05	2,272.07	2,271.08	20
7	707.38	354.2	690.36	689.37	D	2,192.04	1,096.52	2,175.02	2,174.03	19
8	806.45	403.73	789.43	788.44	V	2,077.02	1,039.01	2,059.99	2,059.00	18
9	877.49	439.25	860.46	859.48	A	1,977.95	989.48	1,960.92	1,959.94	17
10	976.56	488.78	959.53	958.55	V	1,906.91	953.96	1,889.88	1,888.90	16
11	1,089.64	545.32	1,072.61	1,071.63	L	1,807.84	904.42	1,790.81	1,789.83	15
12	1,284.63	642.82	1,267.61	1,266.62	D+80	1,694.76	847.88	1,677.73	1,676.75	14
13	1,383.70	692.36	1,366.68	1,365.69	V	1,499.76	750.39	1,482.74	1,481.75	13
14	1,539.80	770.41	1,522.78	1,521.79	R	1,400.70	700.85	1,383.67	1,382.68	12
15	1,652.89	826.95	1,635.86	1,634.88	L	1,244.59	622.8	1,227.57	1,226.58	11
16	1,749.94	875.47	1,732.91	1,731.93	P	1,131.51	566.26	1,114.48	1,113.50	10
17	1,864.97	932.99	1,847.94	1,846.96	D	1,034.46	517.73	1,017.43	1,016.45	9
18	1,921.99	961.5	1,904.96	1,903.98	G	919.43	460.22	902.4	901.42	8
19	2,037.02	1,019.01	2,019.99	2,019.01	N+1	862.41	431.71	845.38	844.4	7
20	2,094.04	1,047.52	2,077.01	2,076.03	G	747.38	374.19	730.36	729.37	6
21	2,207.12	1,104.06	2,190.10	2,189.11	I	690.36	345.68	673.33	672.35	5
22	2,336.16	1,168.59	2,319.14	2,318.15	E	577.28	289.14	560.25	559.27	4
23	2,449.25	1,225.13	2,432.22	2,431.24	L	448.23	224.62	431.21		3
24	2,609.28	1,305.14	2,592.25	2,591.27	C+57	335.15	168.08	318.12		2
25	2,783.39	1,392.20	2,766.36	2,765.38	R	175.12	88.06	158.09		1

Figure 4.5. Annotated MS/MS spectrum confirming phosphorylation of DosR D54 after PknH and acetyl phosphate treatment. (A) MS/MS spectrum of the peptide VPAARPDVAVLdVRLPDGnGIELcR of (m/z 928.5, z=3). Observed *b* and *y* ions, along with neutral-loss fragments (-98 Da), are indicated. (B) Fragmentation map displaying detected ions (red = b; blue = y; green = neutral-loss/derived fragments) confirming site localization at D54.

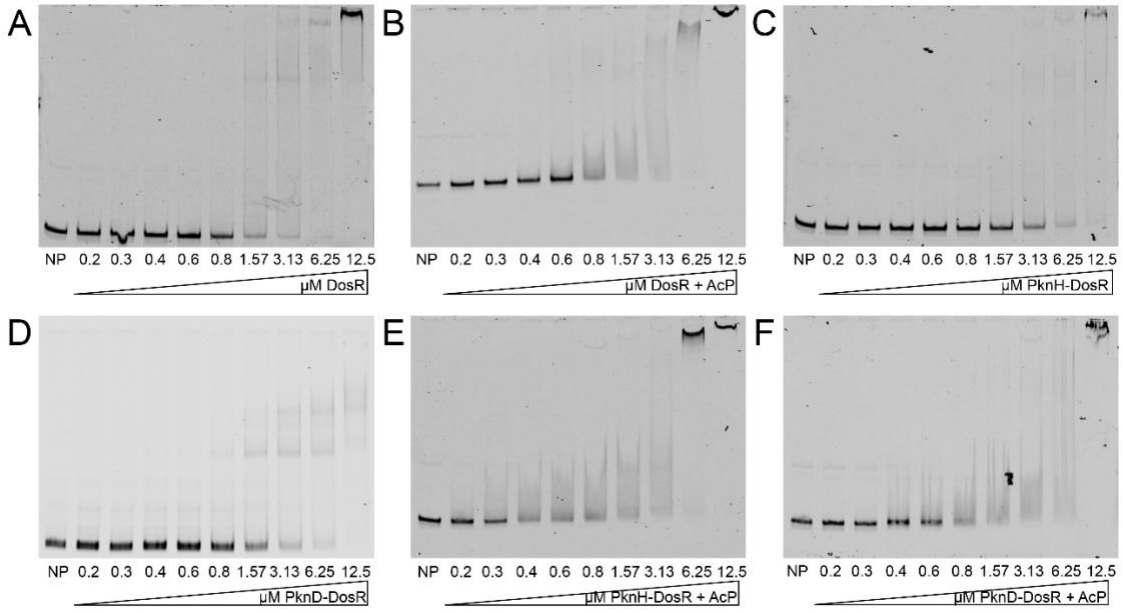

Figure 4.6. Changes in DosR phosphorylation status alter DNA binding affinity to the promoter of its target gene *fdxA*. Electrophoretic mobility shift assays (EMSAs) using purified recombinant C-terminally 6x-His-tagged DosR and IRDye 700-labeled probes for the *fdxA* promoter are shown. A control with no protein ("NP") added is shown for each gel. DosR was added at indicated concentrations for all other lanes. 40 fmoles of *fdxA* promoter DNA was used in each reaction. EMSAs shown are as follows: (A) untreated DosR, (B) DosR incubated with 50 mM acetyl phosphate (AcP), (C) DosR phosphorylated "on-bead" with 1 μM PknH, (D) DosR phosphorylated "on-bead" with 1 μM PknD, (E) DosR phosphorylated "on-bead" with 1 μM PknH, then purified and incubated with 50 mM AcP, and (F) DosR phosphorylated "on-bead" with 1 μM PknD, then purified and incubated with 50 mM AcP. Data are representative of 3 independent experiments.

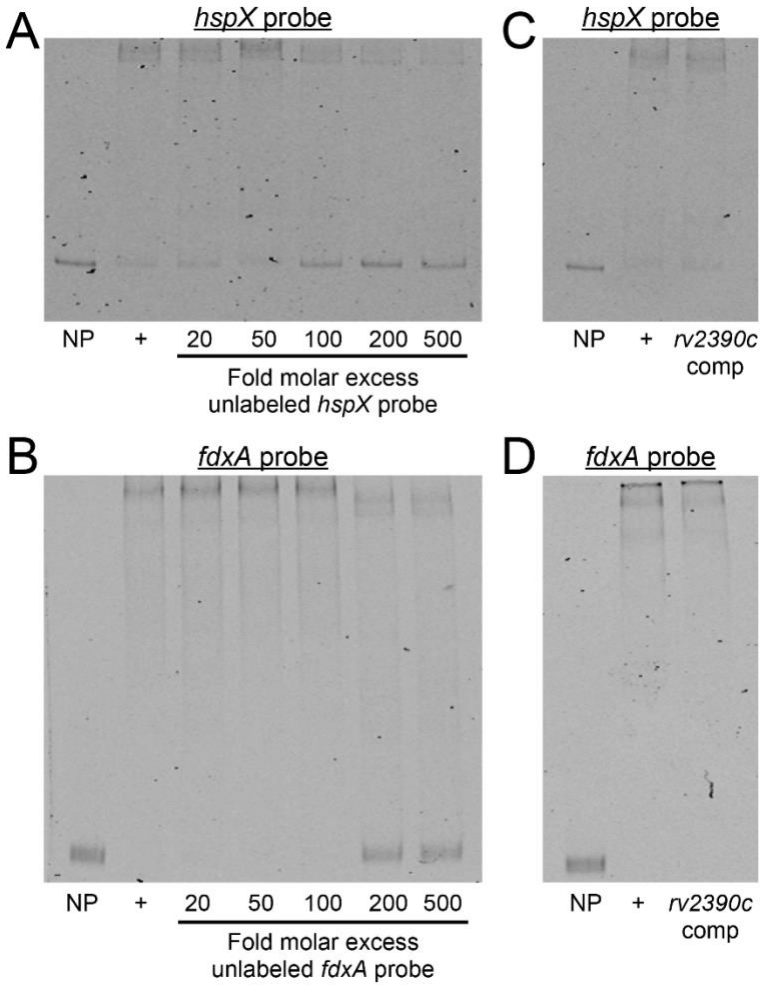

Figure 4.7. DosR binding to the *hspX* and *fdxA* promoters is specific. Electrophoretic mobility shift assays (EMSAs) using purified recombinant C-terminally 6x-His-tagged DosR and IRDye 700-labeled probes for the *hspX* promoter (A and C) and the *fdxA* promoter (B and D) are shown. A control with no protein ("NP") added is shown for each gel. Purified DosR was added at 1.57 μM for all other reactions in the *hspX* promoter EMSAs, and at 6.25 μM for the *fdxA* promoter EMSAs. 1 fmole of each labeled promoter DNA was used in each reaction. "+" are reactions with DosR and the indicated labeled probe, with no competitor unlabeled probe. Where noted, unlabeled specific competitive *hspX* (A) or *fdxA* (B) probes were added at the indicated fold molar excess. In (C) and (D), unlabeled non-specific *rv2390c* promoter probes were added at 200-fold molar excess for reactions in the "*rv2390c* comp" lane.

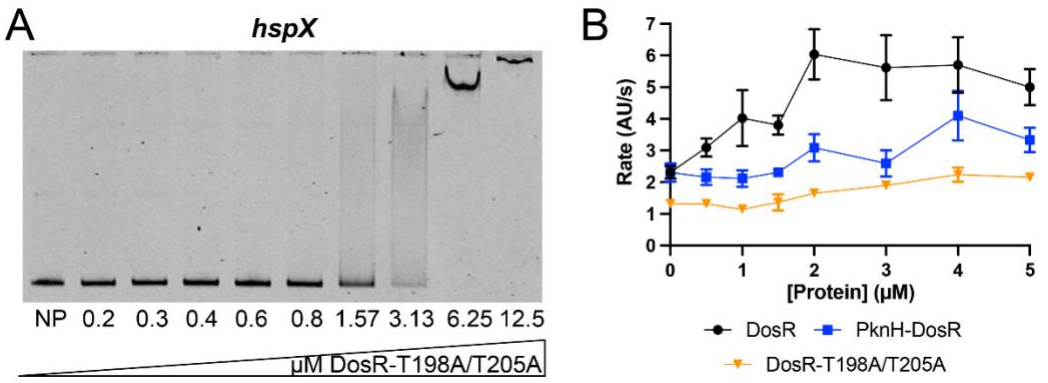

Figure 4.8 Mutation of DosR T198/T205 sites render the protein non-functional. (A) shows an EMSA using purified recombinant C-terminally 6x-His-tagged DosR-T198A/T205A and IRDye 700-labeled probes for the *hspX* promoter. A control with no protein ("NP") added is also shown. DosR-T198A/T205A was added at indicated concentrations for all other lanes. 40 fmoles of *hspX* promoter DNA was used in each reaction. Data are representative of 3 independent experiments. (B) shows a Spinach RNA aptamer assay run with the *fdxA* promoter with different concentrations of indicated DosR protein. The WT DosR and PknH-phosphorylated DosR ("PknH-DosR) data are as shown in Fig 2.4A. Fluorescence (arbitrary units, "AU") was tracked over time on a plate reader, and steady-state rate calculated. Data are shown as means ± SEM from 2-8 experiments. The numerical data underlying the graph shown in this figure are provided in Data File 4.1.

4.1.2 Chapter 2 Supplemental Data Files List

Data file 4.1

Excel workbook. Numerical data underlying graphed average data presented.

Chapter 5: Bibliography

1. Wirth, T., et al., *Origin, spread and demography of the Mycobacterium tuberculosis complex.* PLoS Pathog, 2008. **4**(9): p. e1000160.
2. Hershkovitz, I., et al., *Detection and molecular characterization of 9,000-year-old Mycobacterium tuberculosis from a Neolithic settlement in the Eastern Mediterranean.* PLoS One, 2008. **3**(10): p. e3426.
3. Bloom, B., *Tuberculosis: Pathogenesis, Protection and Control.* Nature Medicine, 1996. **2**(2): p. 244-245.
4. *Tuberculosis: an ongoing global epidemic.* EClinicalMedicine, 2021. **33**: p. 100785.
5. Daniel, T.M., *The history of tuberculosis.* Respir Med, 2006. **100**(11): p. 1862-70.
6. Schatz, A., E. Bugle, and S.A. Waksman, *Streptomycin, a Substance Exhibiting Antibiotic Activity Against Gram-Positive and Gram-Negative Bacteria.∗†.* Proceedings of the Society for Experimental Biology and Medicine, 1944. **55**(1): p. 66-69.
7. Prevention, C.f.D.C.a. *Treating Tuberculosis*. 2025 April 17, 2025 [cited 2026 January 14]; Available from: https://www.cdc.gov/tb/treatment/index.html.
8. *CDC Tuberculosis (TB)*. Clinical Overview of Tuberculosis 2025 [cited 2025 January 6, 2026]; Available from: https://www.cdc.gov/tb/hcp/clinical-overview/index.html.
9. Furin, J., H. Cox, and M. Pai, *Tuberculosis.* Lancet, 2019. **393**(10181): p. 1642-1656.
10. Baykan, A.H., et al., *Extrapulmonary tuberculosıs: an old but resurgent problem.* Insights Imaging, 2022. **13**(1): p. 39.
11. Lin, P.L. and J.L. Flynn, *Understanding latent tuberculosis: a moving target.* J Immunol, 2010. **185**(1): p. 15-22.
12. Hartman-Adams, H., K. Clark, and G. Juckett, *Update on latent tuberculosis infection.* Am Fam Physician, 2014. **89**(11): p. 889-96.
13. *Global Tuberculosis Report 2025*. 2025 [cited 2026 January 6].
14. Lönnroth, K., et al., *Drivers of tuberculosis epidemics: the role of risk factors and social determinants.* Soc Sci Med, 2009. **68**(12): p. 2240-6.
15. Gandhi, N.R., et al., *Multidrug-resistant and extensively drug-resistant tuberculosis: a threat to global control of tuberculosis.* Lancet, 2010. **375**(9728): p. 1830-43.
16. Barros, E.A., et al., *Impacts of the Covid-19 pandemic on the detection and diagnosis of Tuberculosis: Analysis of scientific evidence.* Clinical Epidemiology and Global Health, 2026. **37**: p. 102234.
17. Narain, J.P., M.C. Raviglione, and A. Kochi, *HIV-associated tuberculosis in developing countries: epidemiology and strategies for prevention.* Tuber Lung Dis, 1992. **73**(6): p. 311-21.
18. Zumla, A., et al., *Tuberculosis.* New England Journal of Medicine, 2013. **368**(8): p. 745-755.
19. Teitelbaum, R., et al., *The M Cell as a Portal of Entry to the Lung for the Bacterial Pathogen Mycobacterium tuberculosis.* Immunity, 1999. **10**(6): p. 641-650.

20. Cohen, S.B., et al., *Alveolar Macrophages Provide an Early Mycobacterium tuberculosis Niche and Initiate Dissemination.* Cell Host Microbe, 2018. **24**(3): p. 439-446.e4.
21. Upadhyay, S., E. Mittal, and J.A. Philips, *Tuberculosis and the art of macrophage manipulation.* Pathog Dis, 2018. **76**(4).
22. Sturgill-Koszycki, S., et al., *Lack of acidification in Mycobacterium phagosomes produced by exclusion of the vesicular proton-ATPase.* Science, 1994. **263**(5147): p. 678-81.
23. Wong, D., et al., *Mycobacterium tuberculosis protein tyrosine phosphatase (PtpA) excludes host vacuolar-H+-ATPase to inhibit phagosome acidification.* Proc Natl Acad Sci U S A, 2011. **108**(48): p. 19371-6.
24. Kyei, G.B., et al., *Rab14 is critical for maintenance of Mycobacterium tuberculosis phagosome maturation arrest.* Embo j, 2006. **25**(22): p. 5250-9.
25. Chandra, P., et al., *Mycobacterium tuberculosis Inhibits RAB7 Recruitment to Selectively Modulate Autophagy Flux in Macrophages.* Sci Rep, 2015. **5**: p. 16320.
26. Via, L.E., et al., *Arrest of mycobacterial phagosome maturation is caused by a block in vesicle fusion between stages controlled by rab5 and rab7.* J Biol Chem, 1997. **272**(20): p. 13326-31.
27. Levin, R., S. Grinstein, and J. Canton, *The life cycle of phagosomes: formation, maturation, and resolution.* Immunol Rev, 2016. **273**(1): p. 156-79.
28. Turk, V., et al., *Cysteine cathepsins: from structure, function and regulation to new frontiers.* Biochim Biophys Acta, 2012. **1824**(1): p. 68-88.
29. Riese, R.J., et al., *Cathepsin S activity regulates antigen presentation and immunity.* J Clin Invest, 1998. **101**(11): p. 2351-63.
30. Kinchen, J.M. and K.S. Ravichandran, *Phagosome maturation: going through the acid test.* Nature Reviews Molecular Cell Biology, 2008. **9**(10): p. 781-795.
31. Vidak, E., et al., *Cysteine Cathepsins and their Extracellular Roles: Shaping the Microenvironment.* Cells, 2019. **8**(3).
32. Leon-Sicairos, N., et al., *Strategies of Intracellular Pathogens for Obtaining Iron from the Environment.* Biomed Res Int, 2015. **2015**: p. 476534.
33. Westman, J. and S. Grinstein, *Determinants of Phagosomal pH During Host-Pathogen Interactions.* Front Cell Dev Biol, 2020. **8**: p. 624958.
34. Wayne, L.G. and L.G. Hayes, *An in vitro model for sequential study of shiftdown of Mycobacterium tuberculosis through two stages of nonreplicating persistence.* Infect Immun, 1996. **64**(6): p. 2062-9.
35. Loebel, R.O., E. Shorr, and H.B. Richardson, *The Influence of Foodstuffs upon the Respiratory Metabolism and Growth of Human Tubercle Bacilli.* J Bacteriol, 1933. **26**(2): p. 139-66.
36. Betts, J.C., et al., *Evaluation of a nutrient starvation model of Mycobacterium tuberculosis persistence by gene and protein expression profiling.* Mol Microbiol, 2002. **43**(3): p. 717-31.
37. Gengenbacher, M., et al., *Nutrient-starved, non-replicating Mycobacterium tuberculosis requires respiration, ATP synthase and isocitrate lyase for maintenance of ATP homeostasis and viability.* Microbiology (Reading), 2010. **156**(Pt 1): p. 81-87.

38. Schnappinger, D., et al., *Transcriptional Adaptation of Mycobacterium tuberculosis within Macrophages: Insights into the Phagosomal Environment.* J Exp Med, 2003. **198**(5): p. 693-704.
39. Park, H.D., et al., *Rv3133c/dosR is a transcription factor that mediates the hypoxic response of Mycobacterium tuberculosis.* Mol Microbiol, 2003. **48**(3): p. 833-43.
40. Voskuil, M.I., K.C. Visconti, and G.K. Schoolnik, *Mycobacterium tuberculosis gene expression during adaptation to stationary phase and low-oxygen dormancy.* Tuberculosis (Edinb), 2004. **84**(3-4): p. 218-27.
41. Zahrt, T.C. and V. Deretic, *Mycobacterium tuberculosis signal transduction system required for persistent infections.* Proc Natl Acad Sci U S A, 2001. **98**(22): p. 12706-11.
42. Manganelli, R., et al., *Differential expression of 10 sigma factor genes in Mycobacterium tuberculosis.* Mol Microbiol, 1999. **31**(2): p. 715-24.
43. Samuels, A.N., et al., *Understanding the contribution of metabolism to Mycobacterium tuberculosis drug tolerance.* Front Cell Infect Microbiol, 2022. **12**: p. 958555.
44. Simeone, R., et al., *Cytosolic access of Mycobacterium tuberculosis: critical impact of phagosomal acidification control and demonstration of occurrence in vivo.* PLoS Pathog, 2015. **11**(2): p. e1004650.
45. Augenstreich, J., et al., *ESX-1 and phthiocerol dimycocerosates of Mycobacterium tuberculosis act in concert to cause phagosomal rupture and host cell apoptosis.* Cell Microbiol, 2017. **19**(7).
46. Davis, J.M. and L. Ramakrishnan, *The role of the granuloma in expansion and dissemination of early tuberculous infection.* Cell, 2009. **136**(1): p. 37-49.
47. Bussi, C. and M.G. Gutierrez, *Mycobacterium tuberculosis infection of host cells in space and time.* FEMS Microbiology Reviews, 2019. **43**(4): p. 341-361.
48. de Martino, M., et al., *Immune Response to Mycobacterium tuberculosis: A Narrative Review.* Front Pediatr, 2019. **7**: p. 350.
49. Flynn, J.L., J. Chan, and P.L. Lin, *Macrophages and control of granulomatous inflammation in tuberculosis.* Mucosal Immunol, 2011. **4**(3): p. 271-8.
50. Davis, J.M., et al., *Real-time visualization of mycobacterium-macrophage interactions leading to initiation of granuloma formation in zebrafish embryos.* Immunity, 2002. **17**(6): p. 693-702.
51. Saunders, B.M. and A.M. Cooper, *Restraining mycobacteria: role of granulomas in mycobacterial infections.* Immunol Cell Biol, 2000. **78**(4): p. 334-41.
52. Tiwari, D. and A.R. Martineau, *Inflammation-mediated tissue damage in pulmonary tuberculosis and host-directed therapeutic strategies.* Semin Immunol, 2023. **65**: p. 101672.
53. Kim, M.J., et al., *Caseation of human tuberculosis granulomas correlates with elevated host lipid metabolism.* EMBO Molecular Medicine, 2010. **2**(7): p. 258-274.
54. Driver, E.R., et al., *Evaluation of a mouse model of necrotic granuloma formation using C3HeB/FeJ mice for testing of drugs against Mycobacterium tuberculosis.* Antimicrob Agents Chemother, 2012. **56**(6): p. 3181-95.

55. Ordonez, A.A., et al., *Mouse model of pulmonary cavitary tuberculosis and expression of matrix metalloproteinase-9.* Dis Model Mech, 2016. **9**(7): p. 779-88.
56. Moreira-Teixeira, L., et al., *T Cell-Derived IL-10 Impairs Host Resistance to Mycobacterium tuberculosis Infection.* J Immunol, 2017. **199**(2): p. 613-623.
57. Voskuil, M.I., et al., *The response of mycobacterium tuberculosis to reactive oxygen and nitrogen species.* Front Microbiol, 2011. **2**: p. 105.
58. Ehrt, S. and D. Schnappinger, *Mycobacterial survival strategies in the phagosome: defence against host stresses.* Cell Microbiol, 2009. **11**(8): p. 1170-8.
59. Tan, S., et al., *Mycobacterium tuberculosis responds to chloride and pH as synergistic cues to the immune status of its host cell.* PLoS Pathog, 2013. **9**(4): p. e1003282.
60. MacGilvary, N.J., Y.L. Kevorkian, and S. Tan, *Potassium response and homeostasis in Mycobacterium tuberculosis modulates environmental adaptation and is important for host colonization.* PLoS Pathog, 2019. **15**(2): p. e1007591.
61. Ramakrishnan, L., *Revisiting the role of the granuloma in tuberculosis.* Nature Reviews Immunology, 2012. **12**(5): p. 352-366.
62. Via, L.E., et al., *Tuberculous granulomas are hypoxic in guinea pigs, rabbits, and nonhuman primates.* Infect Immun, 2008. **76**(6): p. 2333-40.
63. Kumar, A., et al., *Redox homeostasis in mycobacteria: the key to tuberculosis control?* Expert Rev Mol Med, 2011. **13**: p. e39.
64. Chinta, K.C., et al., *The emerging role of gasotransmitters in the pathogenesis of tuberculosis.* Nitric Oxide, 2016. **59**: p. 28-41.
65. Kumar, A., et al., *Mycobacterium tuberculosis DosS is a redox sensor and DosT is a hypoxia sensor.* Proc Natl Acad Sci U S A, 2007. **104**(28): p. 11568-73.
66. Leistikow, R.L., et al., *The Mycobacterium tuberculosis DosR regulon assists in metabolic homeostasis and enables rapid recovery from nonrespiring dormancy.* J Bacteriol, 2010. **192**(6): p. 1662-70.
67. Vila-del Sol, V., M.D. Díaz-Muñoz, and M. Fresno, *Requirement of tumor necrosis factor alpha and nuclear factor-kappaB in the induction by IFN-gamma of inducible nitric oxide synthase in macrophages.* J Leukoc Biol, 2007. **81**(1): p. 272-83.
68. Cooper, A.M., et al., *Disseminated tuberculosis in interferon gamma gene-disrupted mice.* J Exp Med, 1993. **178**(6): p. 2243-7.
69. Förstermann, U. and W.C. Sessa, *Nitric oxide synthases: regulation and function.* Eur Heart J, 2012. **33**(7): p. 829-37, 837a-837d.
70. Scanga, C.A., et al., *The inducible nitric oxide synthase locus confers protection against aerogenic challenge of both clinical and laboratory strains of Mycobacterium tuberculosis in mice.* Infect Immun, 2001. **69**(12): p. 7711-7.
71. Schairer, D.O., et al., *The potential of nitric oxide releasing therapies as antimicrobial agents.* Virulence, 2012. **3**(3): p. 271-9.
72. Rong, F., et al., *Nitric Oxide-Releasing Polymeric Materials for Antimicrobial Applications: A Review.* Antioxidants (Basel), 2019. **8**(11).
73. Boon, C. and T. Dick, *Mycobacterium bovis BCG response regulator essential for hypoxic dormancy.* J Bacteriol, 2002. **184**(24): p. 6760-7.
74. Shaku, M.T. and W.R. Bishai, *Mycobacterium tuberculosis: A Pathogen That Can Hold Its Breath a Long Time.* Am J Respir Crit Care Med, 2022. **206**(1): p. 10-12.

75. Sherman, D.R., et al., *Regulation of the Mycobacterium tuberculosis hypoxic response gene encoding alpha -crystallin.* Proc Natl Acad Sci U S A, 2001. **98**(13): p. 7534-9.
76. Desjardin, L.E., et al., *Microaerophilic induction of the alpha-crystallin chaperone protein homologue (hspX) mRNA of Mycobacterium tuberculosis.* J Bacteriol, 2001. **183**(18): p. 5311-6.
77. Voskuil, M.I., et al., *Inhibition of respiration by nitric oxide induces a Mycobacterium tuberculosis dormancy program.* J Exp Med, 2003. **198**(5): p. 705-13.
78. Rustad, T.R., et al., *The Enduring Hypoxic Response of Mycobacterium tuberculosis.* PLOS ONE, 2008. **3**(1): p. e1502.
79. Daniel, J., et al., *Induction of a novel class of diacylglycerol acyltransferases and triacylglycerol accumulation in Mycobacterium tuberculosis as it goes into a dormancy-like state in culture.* J Bacteriol, 2004. **186**(15): p. 5017-30.
80. Deb, C., et al., *A novel in vitro multiple-stress dormancy model for Mycobacterium tuberculosis generates a lipid-loaded, drug-tolerant, dormant pathogen.* PLoS One, 2009. **4**(6): p. e6077.
81. Stevanin, T.M., et al., *Flavohemoglobin Hmp affords inducible protection for Escherichia coli respiration, catalyzed by cytochromes bo' or bd, from nitric oxide.* J Biol Chem, 2000. **275**(46): p. 35868-75.
82. Stevanin, T.M., et al., *Flavohemoglobin Hmp protects Salmonella enterica serovar typhimurium from nitric oxide-related killing by human macrophages.* Infect Immun, 2002. **70**(8): p. 4399-405.
83. Gardner, P.R., et al., *Nitric oxide dioxygenase: an enzymic function for flavohemoglobin.* Proc Natl Acad Sci U S A, 1998. **95**(18): p. 10378-83.
84. Gardner, A.M., R.A. Helmick, and P.R. Gardner, *Flavorubredoxin, an Inducible Catalyst for Nitric Oxide Reduction and Detoxification in Escherichia coli *.* Journal of Biological Chemistry, 2002. **277**(10): p. 8172-8177.
85. Hutchings, M.I., N. Mandhana, and S. Spiro, *The NorR protein of Escherichia coli activates expression of the flavorubredoxin gene norV in response to reactive nitrogen species.* J Bacteriol, 2002. **184**(16): p. 4640-3.
86. Justino, M.C., et al., *Escherichia coli Di-iron YtfE Protein Is Necessary for the Repair of Stress-damaged Iron-Sulfur Clusters*.* Journal of Biological Chemistry, 2007. **282**(14): p. 10352-10359.
87. Overton, T.W., et al., *Widespread distribution in pathogenic bacteria of di-iron proteins that repair oxidative and nitrosative damage to iron-sulfur centers.* J Bacteriol, 2008. **190**(6): p. 2004-13.
88. Tucker, N.P., et al., *The transcriptional repressor protein NsrR senses nitric oxide directly via a [2Fe-2S] cluster.* PLoS One, 2008. **3**(11): p. e3623.
89. Filenko, N., et al., *The NsrR regulon of Escherichia coli K-12 includes genes encoding the hybrid cluster protein and the periplasmic, respiratory nitrite reductase.* J Bacteriol, 2007. **189**(12): p. 4410-7.
90. Sershen, C.L., S.J. Plimpton, and E.E. May, *Oxygen Modulates the Effectiveness of Granuloma Mediated Host Response to Mycobacterium tuberculosis: A Multiscale Computational Biology Approach.* Front Cell Infect Microbiol, 2016. **6**: p. 6.

91. Datta, M., et al., *Mathematical Model of Oxygen Transport in Tuberculosis Granulomas.* Ann Biomed Eng, 2016. **44**(4): p. 863-72.
92. Yates, R.M., A. Hermetter, and D.G. Russell, *The kinetics of phagosome maturation as a function of phagosome/lysosome fusion and acquisition of hydrolytic activity.* Traffic, 2005. **6**(5): p. 413-20.
93. Buter, J., et al., *Mycobacterium tuberculosis releases an antacid that remodels phagosomes.* Nature Chemical Biology, 2019. **15**(9): p. 889-899.
94. Vandal, O.H., et al., *A membrane protein preserves intrabacterial pH in intraphagosomal Mycobacterium tuberculosis.* Nat Med, 2008. **14**(8): p. 849-54.
95. Piddington, D.L., A. Kashkouli, and N.A. Buchmeier, *Growth of Mycobacterium tuberculosis in a defined medium is very restricted by acid pH and Mg(2+) levels.* Infect Immun, 2000. **68**(8): p. 4518-22.
96. Baker, J.J., B.K. Johnson, and R.B. Abramovitch, *Slow growth of Mycobacterium tuberculosis at acidic pH is regulated by phoPR and host-associated carbon sources.* Mol Microbiol, 2014. **94**(1): p. 56-69.
97. Chiaradia, L., et al., *Dissecting the mycobacterial cell envelope and defining the composition of the native mycomembrane.* Scientific Reports, 2017. **7**(1): p. 12807.
98. Hoffmann, C., et al., *Disclosure of the mycobacterial outer membrane: cryo-electron tomography and vitreous sections reveal the lipid bilayer structure.* Proc Natl Acad Sci U S A, 2008. **105**(10): p. 3963-7.
99. Zuber, B., et al., *Direct visualization of the outer membrane of mycobacteria and corynebacteria in their native state.* J Bacteriol, 2008. **190**(16): p. 5672-80.
100. Vandal, O.H., C.F. Nathan, and S. Ehrt, *Acid resistance in Mycobacterium tuberculosis.* J Bacteriol, 2009. **191**(15): p. 4714-21.
101. Rohde, K.H., R.B. Abramovitch, and D.G. Russell, *Mycobacterium tuberculosis Invasion of Macrophages: Linking Bacterial Gene Expression to Environmental Cues.* Cell Host & Microbe, 2007. **2**(5): p. 352-364.
102. Martin, C., et al., *The live Mycobacterium tuberculosis phoP mutant strain is more attenuated than BCG and confers protective immunity against tuberculosis in mice and guinea pigs.* Vaccine, 2006. **24**(17): p. 3408-3419.
103. Yunos, N.M., et al., *Bench-to-bedside review: Chloride in critical illness.* Crit Care, 2010. **14**(4): p. 226.
104. Raut, Satish K., et al., *Chloride ions in health and disease.* Bioscience Reports, 2024. **44**(5).
105. Lukasiak, A. and M. Zajac, *The Distribution and Role of the CFTR Protein in the Intracellular Compartments.* Membranes, 2021. **11**(11): p. 804.
106. Jentsch, T.J., T. Maritzen, and A.A. Zdebik, *Chloride channel diseases resulting from impaired transepithelial transport or vesicular function.* J Clin Invest, 2005. **115**(8): p. 2039-46.
107. Miller, F.J., Jr., et al., *Cytokine activation of nuclear factor kappa B in vascular smooth muscle cells requires signaling endosomes containing Nox1 and ClC-3.* Circ Res, 2007. **101**(7): p. 663-71.
108. Nauseef, W.M., *Myeloperoxidase in human neutrophil host defence.* Cell Microbiol, 2014. **16**(8): p. 1146-55.

109. Sonawane, N.D., J.R. Thiagarajah, and A.S. Verkman, *Chloride concentration in endosomes measured using a ratioable fluorescent Cl- indicator: evidence for chloride accumulation during acidification.* J Biol Chem, 2002. **277**(7): p. 5506-13.
110. Zacchia, M., et al., *Potassium: From Physiology to Clinical Implications.* Kidney Dis (Basel), 2016. **2**(2): p. 72-9.
111. Edwards, G. and A.H. Weston, *The role of potassium channels in excitable cells.* Diabetes Res Clin Pract, 1995. **28 Suppl**: p. S57-66.
112. Nielsen, O.B. and F.V. de Paoli, *Regulation of Na+-K+ homeostasis and excitability in contracting muscles: implications for fatigue.* Appl Physiol Nutr Metab, 2007. **32**(5): p. 974-84.
113. Warth, R., *Potassium channels in epithelial transport.* Pflugers Arch, 2003. **446**(5): p. 505-13.
114. Palmer, B.F., *Regulation of Potassium Homeostasis.* Clin J Am Soc Nephrol, 2015. **10**(6): p. 1050-60.
115. Feske, S., H. Wulff, and E.Y. Skolnik, *Ion channels in innate and adaptive immunity.* Annu Rev Immunol, 2015. **33**: p. 291-353.
116. Di, A., et al., *The TWIK2 Potassium Efflux Channel in Macrophages Mediates NLRP3 Inflammasome-Induced Inflammation.* Immunity, 2018. **49**(1): p. 56-65.e4.
117. Muñoz-Planillo, R., et al., *K^+ efflux is the common trigger of NLRP3 inflammasome activation by bacterial toxins and particulate matter.* Immunity, 2013. **38**(6): p. 1142-53.
118. Liu, Y., et al., *Potassium transport of Salmonella is important for type III secretion and pathogenesis.* Microbiology (Reading), 2013. **159**(Pt 8): p. 1705-1719.
119. Su, J., et al., *The potassium transporter Trk and external potassium modulate Salmonella enterica protein secretion and virulence.* Infect Immun, 2009. **77**(2): p. 667-75.
120. Gries, C.M., et al., *The Ktr potassium transport system in Staphylococcus aureus and its role in cell physiology, antimicrobial resistance and pathogenesis.* Mol Microbiol, 2013. **89**(4): p. 760-73.
121. Steyn, A.J., J. Joseph, and B.R. Bloom, *Interaction of the sensor module of Mycobacterium tuberculosis H37Rv KdpD with members of the Lpr family.* Mol Microbiol, 2003. **47**(4): p. 1075-89.
122. Hoch, J.A., *Two-component and phosphorelay signal transduction.* Curr Opin Microbiol, 2000. **3**(2): p. 165-70.
123. Stock, A.M., V.L. Robinson, and P.N. Goudreau, *Two-component signal transduction.* Annu Rev Biochem, 2000. **69**: p. 183-215.
124. Wuichet, K., B.J. Cantwell, and I.B. Zhulin, *Evolution and phyletic distribution of two-component signal transduction systems.* Curr Opin Microbiol, 2010. **13**(2): p. 219-25.
125. West, A.H. and A.M. Stock, *Histidine kinases and response regulator proteins in two-component signaling systems.* Trends Biochem Sci, 2001. **26**(6): p. 369-76.
126. Jung, K., et al., *Histidine kinases and response regulators in networks.* Curr Opin Microbiol, 2012. **15**(2): p. 118-24.

127. Makino, K., et al., *Regulation of the phosphate regulon of Escherichia coli. Activation of pstS transcription by PhoB protein in vitro.* J Mol Biol, 1988. **203**(1): p. 85-95.
128. Russo, F.D. and T.J. Silhavy, *EnvZ controls the concentration of phosphorylated OmpR to mediate osmoregulation of the porin genes.* J Mol Biol, 1991. **222**(3): p. 567-80.
129. Miller, S.I., A.M. Kukral, and J.J. Mekalanos, *A two-component regulatory system (phoP phoQ) controls Salmonella typhimurium virulence.* Proc Natl Acad Sci U S A, 1989. **86**(13): p. 5054-8.
130. Bina, J., et al., *ToxR regulon of Vibrio cholerae and its expression in vibrios shed by cholera patients.* Proc Natl Acad Sci U S A, 2003. **100**(5): p. 2801-6.
131. Walters, S.B., et al., *The Mycobacterium tuberculosis PhoPR two-component system regulates genes essential for virulence and complex lipid biosynthesis.* Mol Microbiol, 2006. **60**(2): p. 312-30.
132. Foo, Y.H., et al., *Cytoplasmic sensing by the inner membrane histidine kinase EnvZ.* Prog Biophys Mol Biol, 2015. **118**(3): p. 119-29.
133. Gerken, H., et al., *Effects of pleiotropic ompR and envZ alleles of Escherichia coli on envelope stress and antibiotic sensitivity.* J Bacteriol, 2024. **206**(6): p. e0017224.
134. Chakraborty, S. and L.J. Kenney, *A New Role of OmpR in Acid and Osmotic Stress in Salmonella and E. coli.* Front Microbiol, 2018. **9**: p. 2656.
135. Groisman, E.A., *The pleiotropic two-component regulatory system PhoP-PhoQ.* J Bacteriol, 2001. **183**(6): p. 1835-42.
136. Gao, X., et al., *The Effect of the PhoP/PhoQ System on the Regulation of Multi-Stress Adaptation Induced by Acid Stress in Salmonella Typhimurium.* Foods, 2024. **13**(10): p. 1533.
137. Kato, A. and E.A. Groisman, *The PhoQ/PhoP regulatory network of Salmonella enterica.* Adv Exp Med Biol, 2008. **631**: p. 7-21.
138. Wong, S.M., et al., *Modulation of expression of the ToxR regulon in Vibrio cholerae by a member of the two-component family of response regulators.* Infect Immun, 1998. **66**(12): p. 5854-61.
139. Ashby, M.K., *Survey of the number of two-component response regulator genes in the complete and annotated genome sequences of prokaryotes.* FEMS Microbiol Lett, 2004. **231**(2): p. 277-81.
140. Mehra, S., et al., *The DosR Regulon Modulates Adaptive Immunity and Is Essential for Mycobacterium tuberculosis Persistence.* Am J Respir Crit Care Med, 2015. **191**(10): p. 1185-96.
141. Elsen, S., et al., *RegB/RegA, a highly conserved redox-responding global two-component regulatory system.* Microbiol Mol Biol Rev, 2004. **68**(2): p. 263-79.
142. Haydel, S.E., et al., *The prrAB two-component system is essential for Mycobacterium tuberculosis viability and is induced under nitrogen-limiting conditions.* J Bacteriol, 2012. **194**(2): p. 354-61.
143. Giacalone, D., et al., *PrrA modulates Mycobacterium tuberculosis response to multiple environmental cues and is critically regulated by serine/threonine protein kinases.* PLOS Genetics, 2022. **18**(8): p. e1010331.

144. Maarsingh, J.D., et al., *Comparative transcriptomics reveals PrrAB-mediated control of metabolic, respiration, energy-generating, and dormancy pathways in Mycobacterium smegmatis.* BMC Genomics, 2019. **20**(1): p. 942.
145. Haller, Y.A., et al., *M. tuberculosis PrrA binds the dosR promoter and regulates mycobacterial adaptation to hypoxia.* Tuberculosis (Edinb), 2024. **148**: p. 102531.
146. Solans, L., et al., *The PhoP-Dependent ncRNA Mcr7 Modulates the TAT Secretion System in Mycobacterium tuberculosis.* PLOS Pathogens, 2014. **10**(5): p. e1004183.
147. Gonzalo-Asensio, J., et al., *PhoP: A Missing Piece in the Intricate Puzzle of Mycobacterium tuberculosis Virulence.* PLOS ONE, 2008. **3**(10): p. e3496.
148. Cholo, M.C., et al., *Role of the kdpDE Regulatory Operon of Mycobacterium tuberculosis in Modulating Bacterial Growth in vitro.* Front Genet, 2021. **12**: p. 698875.
149. Janczarek, M., et al., *Hanks-Type Serine/Threonine Protein Kinases and Phosphatases in Bacteria: Roles in Signaling and Adaptation to Various Environments.* Int J Mol Sci, 2018. **19**(10).
150. Frando, A., et al., *The Mycobacterium tuberculosis protein O-phosphorylation landscape.* Nature Microbiology, 2023. **8**(3): p. 548-561.
151. Hanks, S.K. and T. Hunter, *Protein kinases 6. The eukaryotic protein kinase superfamily: kinase (catalytic) domain structure and classification.* Faseb j, 1995. **9**(8): p. 576-96.
152. Nováková, L., et al., *Identification of multiple substrates of the StkP Ser/Thr protein kinase in Streptococcus pneumoniae.* J Bacteriol, 2010. **192**(14): p. 3629-38.
153. Beilharz, K., et al., *Control of cell division in Streptococcus pneumoniae by the conserved Ser/Thr protein kinase StkP.* Proc Natl Acad Sci U S A, 2012. **109**(15): p. E905-13.
154. Wamp, S., et al., *PrkA controls peptidoglycan biosynthesis through the essential phosphorylation of ReoM.* Elife, 2020. **9**.
155. Sassetti, C.M., D.H. Boyd, and E.J. Rubin, *Genes required for mycobacterial growth defined by high density mutagenesis.* Mol Microbiol, 2003. **48**(1): p. 77-84.
156. Mir, M., et al., *The extracytoplasmic domain of the Mycobacterium tuberculosis Ser/Thr kinase PknB binds specific muropeptides and is required for PknB localization.* PLoS Pathog, 2011. **7**(7): p. e1002182.
157. Gee, C.L., et al., *A phosphorylated pseudokinase complex controls cell wall synthesis in mycobacteria.* Sci Signal, 2012. **5**(208): p. ra7.
158. Shah, I.M., et al., *A eukaryotic-like Ser/Thr kinase signals bacteria to exit dormancy in response to peptidoglycan fragments.* Cell, 2008. **135**(3): p. 486-96.
159. Kelliher, J.L., et al., *PASTA kinase-dependent control of peptidoglycan synthesis via ReoM is required for cell wall stress responses, cytosolic survival, and virulence in Listeria monocytogenes.* PLoS Pathog, 2021. **17**(10): p. e1009881.
160. Zeng, J., et al., *Protein kinases PknA and PknB independently and coordinately regulate essential Mycobacterium tuberculosis physiologies and antimicrobial susceptibility.* PLoS Pathog, 2020. **16**(4): p. e1008452.

161. Gómez-Velasco, A., et al., *Disruption of the serine/threonine protein kinase H affects phthiocerol dimycocerosates synthesis in Mycobacterium tuberculosis.* Microbiology (Reading), 2013. **159**(Pt 4): p. 726-736.
162. Papavinasasundaram, K.G., et al., *Deletion of the Mycobacterium tuberculosis pknH gene confers a higher bacillary load during the chronic phase of infection in BALB/c mice.* J Bacteriol, 2005. **187**(16): p. 5751-60.
163. Molle, V., et al., *An FHA phosphoprotein recognition domain mediates protein EmbR phosphorylation by PknH, a Ser/Thr protein kinase from Mycobacterium tuberculosis.* Biochemistry, 2003. **42**(51): p. 15300-9.
164. Zhang, N., et al., *The Emb proteins of mycobacteria direct arabinosylation of lipoarabinomannan and arabinogalactan via an N-terminal recognition region and a C-terminal synthetic region.* Mol Microbiol, 2003. **50**(1): p. 69-76.
165. Escuyer, V.E., et al., *The role of the embA and embB gene products in the biosynthesis of the terminal hexaarabinofuranosyl motif of Mycobacterium smegmatis arabinogalactan.* J Biol Chem, 2001. **276**(52): p. 48854-62.
166. Hatzios, S.K., et al., *Osmosensory signaling in Mycobacterium tuberculosis mediated by a eukaryotic-like Ser/Thr protein kinase.* Proc Natl Acad Sci U S A, 2013. **110**(52): p. E5069-77.
167. Be, N.A., W.R. Bishai, and S.K. Jain, *Role of Mycobacterium tuberculosis pknD in the Pathogenesis of central nervous system tuberculosis.* BMC Microbiology, 2012. **12**(1): p. 7.
168. Libby, E.A., L.A. Goss, and J. Dworkin, *The Eukaryotic-Like Ser/Thr Kinase PrkC Regulates the Essential WalRK Two-Component System in Bacillus subtilis.* PLoS Genet, 2015. **11**(6): p. e1005275.
169. Horstmann, N., et al., *Dual-site phosphorylation of the control of virulence regulator impacts group a streptococcal global gene expression and pathogenesis.* PLoS Pathog, 2014. **10**(5): p. e1004088.
170. Chao, J.D., et al., *Convergence of Ser/Thr and two-component signaling to coordinate expression of the dormancy regulon in Mycobacterium tuberculosis.* J Biol Chem, 2010. **285**(38): p. 29239-46.
171. Chan, J., et al., *Killing of virulent Mycobacterium tuberculosis by reactive nitrogen intermediates produced by activated murine macrophages.* J Exp Med, 1992. **175**(4): p. 1111-22.
172. Ohno, H., et al., *The effects of reactive nitrogen intermediates on gene expression in Mycobacterium tuberculosis.* Cell Microbiol, 2003. **5**(9): p. 637-48.
173. Cadena, A.M., S.M. Fortune, and J.L. Flynn, *Heterogeneity in tuberculosis.* Nat Rev Immunol, 2017. **17**(11): p. 691-702.
174. Lavin, R.C. and S. Tan, *Spatial relationships of intra-lesion heterogeneity in Mycobacterium tuberculosis microenvironment, replication status, and drug efficacy.* bioRxiv, 2021: p. 2021.11.08.467819.
175. Lenaerts, A., C.E. Barry, 3rd, and V. Dartois, *Heterogeneity in tuberculosis pathology, microenvironments and therapeutic responses.* Immunol Rev, 2015. **264**(1): p. 288-307.
176. Manina, G., N. Dhar, and J.D. McKinney, *Stress and host immunity amplify Mycobacterium tuberculosis phenotypic heterogeneity and induce nongrowing metabolically active forms.* Cell Host Microbe, 2015. **17**(1): p. 32-46.

177. Walter, N.D., et al., *Lung microenvironments harbor Mycobacterium tuberculosis phenotypes with distinct treatment responses.* Antimicrob Agents Chemother, 2023. **67**(9): p. e0028423.
178. Parish, T., *Two-Component Regulatory Systems of Mycobacteria.* Microbiol Spectr, 2014. **2**(1): p. Mgm2-0010-2013.
179. Buschiazzo, A. and F. Trajtenberg, *Two-Component Sensing and Regulation: How Do Histidine Kinases Talk with Response Regulators at the Molecular Level?* Annu Rev Microbiol, 2019. **73**: p. 507-528.
180. Alm, E., K. Huang, and A. Arkin, *The evolution of two-component systems in bacteria reveals different strategies for niche adaptation.* PLoS Comput Biol, 2006. **2**(11): p. e143.
181. Koretke, K.K., et al., *Evolution of two-component signal transduction.* Mol Biol Evol, 2000. **17**(12): p. 1956-70.
182. Galperin, M.Y., *A census of membrane-bound and intracellular signal transduction proteins in bacteria: bacterial IQ, extroverts and introverts.* BMC Microbiol, 2005. **5**: p. 35.
183. Ulrich, L.E. and I.B. Zhulin, *The MiST2 database: a comprehensive genomics resource on microbial signal transduction.* Nucleic Acids Res, 2010. **38**(Database issue): p. D401-7.
184. Skerker, J.M., et al., *Two-component signal transduction pathways regulating growth and cell cycle progression in a bacterium: a system-level analysis.* PLoS Biol, 2005. **3**(10): p. e334.
185. Ewann, F., et al., *Transient requirement of the PrrA-PrrB two-component system for early intracellular multiplication of Mycobacterium tuberculosis.* Infect Immun, 2002. **70**(5): p. 2256-63.
186. Prisic, S. and R.N. Husson, *Mycobacterium tuberculosis Serine/Threonine Protein Kinases.* Microbiol Spectr, 2014. **2**(5).
187. Nagarajan, S.N., C. Lenoir, and C. Grangeasse, *Recent advances in bacterial signaling by serine/threonine protein kinases.* Trends Microbiol, 2022. **30**(6): p. 553-566.
188. Dworkin, J., *Ser/Thr phosphorylation as a regulatory mechanism in bacteria.* Curr Opin Microbiol, 2015. **24**: p. 47-52.
189. Stancik, I.A., et al., *Serine/Threonine Protein Kinases from Bacteria, Archaea and Eukarya Share a Common Evolutionary Origin Deeply Rooted in the Tree of Life.* J Mol Biol, 2018. **430**(1): p. 27-32.
190. Prisic, S., et al., *Extensive phosphorylation with overlapping specificity by Mycobacterium tuberculosis serine/threonine protein kinases.* Proc Natl Acad Sci U S A, 2010. **107**(16): p. 7521-6.
191. Leasure, C.S., et al., *Maintenance of heme homeostasis in Staphylococcus aureus through post-translational regulation of glutamyl-tRNA reductase.* J Bacteriol, 2023. **205**(9): p. e0017123.
192. Cole, S.T., et al., *Deciphering the biology of Mycobacterium tuberculosis from the complete genome sequence.* Nature, 1998. **393**(6685): p. 537-44.
193. Luu, L.D.W., et al., *Comparative Phosphoproteomics of Classical Bordetellae Elucidates the Potential Role of Serine, Threonine and Tyrosine Phosphorylation*

in Bordetella Biology and Virulence. Front Cell Infect Microbiol, 2021. **11**: p. 660280.
194. Piñas, G.E., et al., *Crosstalk between the serine/threonine kinase StkP and the response regulator ComE controls the stress response and intracellular survival of Streptococcus pneumoniae.* PLoS Pathog, 2018. **14**(6): p. e1007118.
195. Kalantari, A., et al., *Serine/threonine/tyrosine phosphorylation regulates DNA binding of bacterial transcriptional regulators.* Microbiology (Reading), 2015. **161**(9): p. 1720-1729.
196. Rajagopal, L., et al., *Regulation of cytotoxin expression by converging eukaryotic-type and two-component signalling mechanisms in Streptococcus agalactiae.* Mol Microbiol, 2006. **62**(4): p. 941-57.
197. Canova, M.J., et al., *A novel mode of regulation of the Staphylococcus aureus Vancomycin-resistance-associated response regulator VraR mediated by Stk1 protein phosphorylation.* Biochem Biophys Res Commun, 2014. **447**(1): p. 165-71.
198. Mishra, A.K., et al., *Dual phosphorylation in response regulator protein PrrA is crucial for intracellular survival of mycobacteria consequent upon transcriptional activation.* Biochem J, 2017. **474**(24): p. 4119-4136.
199. Chauhan, S. and J.S. Tyagi, *Cooperative binding of phosphorylated DevR to upstream sites is necessary and sufficient for activation of the Rv3134c-devRS operon in Mycobacterium tuberculosis: implication in the induction of DevR target genes.* J Bacteriol, 2008. **190**(12): p. 4301-12.
200. Lin, W.J., et al., *Threonine phosphorylation prevents promoter DNA binding of the Group B Streptococcus response regulator CovR.* Mol Microbiol, 2009. **71**(6): p. 1477-95.
201. Singh, A., et al., *Dissecting virulence pathways of Mycobacterium tuberculosis through protein-protein association.* Proc Natl Acad Sci U S A, 2006. **103**(30): p. 11346-51.
202. Roberts, D.M., et al., *Two sensor kinases contribute to the hypoxic response of Mycobacterium tuberculosis.* J Biol Chem, 2004. **279**(22): p. 23082-7.
203. Saini, D.K., et al., *DevR-DevS is a bona fide two-component system of Mycobacterium tuberculosis that is hypoxia-responsive in the absence of the DNA-binding domain of DevR.* Microbiology (Reading), 2004. **150**(Pt 4): p. 865-875.
204. Gupta, R.K., S. Chauhan, and J.S. Tyagi, *K182G substitution in DevR or C_8G mutation in the Dev box impairs protein-DNA interaction and abrogates DevR-mediated gene induction in Mycobacterium tuberculosis.* Febs j, 2011. **278**(12): p. 2131-9.
205. Gautam, U.S., et al., *DosS Is required for the complete virulence of mycobacterium tuberculosis in mice with classical granulomatous lesions.* Am J Respir Cell Mol Biol, 2015. **52**(6): p. 708-16.
206. Jacob, H., et al., *Distinct Interaction Mechanism of RNA Polymerase and ResD at Proximal and Distal Subsites for Transcription Activation of Nitrite Reductase in Bacillus subtilis.* J Bacteriol, 2022. **204**(2): p. e0043221.

207. Galburt, E.A., *The calculation of transcript flux ratios reveals single regulatory mechanisms capable of activation and repression.* Proc Natl Acad Sci U S A, 2018. **115**(50): p. E11604-e11613.
208. Jensen, D., et al., *High-throughput, fluorescent-aptamer-based measurements of steady-state transcription rates for the Mycobacterium tuberculosis RNA polymerase.* Nucleic Acids Res, 2023. **51**(19): p. e99.
209. Ruiz Manzano, A., D. Jensen, and E.A. Galburt, *Regulation of steady state ribosomal transcription in Mycobacterium tuberculosis: Intersection of sigma subunits, superhelicity, and transcription factors.* J Biol Chem, 2025. **301**(8): p. 110369.
210. Carette, X., et al., *Multisystem Analysis of Mycobacterium tuberculosis Reveals Kinase-Dependent Remodeling of the Pathogen-Environment Interface.* mBio, 2018. **9**(2).
211. Wisedchaisri, G., et al., *Crystal structures of the response regulator DosR from Mycobacterium tuberculosis suggest a helix rearrangement mechanism for phosphorylation activation.* J Mol Biol, 2008. **378**(1): p. 227-42.
212. Wisedchaisri, G., et al., *Structures of Mycobacterium tuberculosis DosR and DosR-DNA complex involved in gene activation during adaptation to hypoxic latency.* J Mol Biol, 2005. **354**(3): p. 630-41.
213. Vashist, A., et al., *The α10 helix of DevR, the Mycobacterium tuberculosis dormancy response regulator, regulates its DNA binding and activity.* Febs j, 2016. **283**(7): p. 1286-99.
214. He, X., L. Wang, and S. Wang, *Structural basis of DNA sequence recognition by the response regulator PhoP in Mycobacterium tuberculosis.* Scientific Reports, 2016. **6**(1): p. 24442.
215. Wang, S., J. Engohang-Ndong, and I. Smith, *Structure of the DNA-binding domain of the response regulator PhoP from Mycobacterium tuberculosis.* Biochemistry, 2007. **46**(51): p. 14751-61.
216. Alber, T., *Signaling mechanisms of the Mycobacterium tuberculosis receptor Ser/Thr protein kinases.* Curr Opin Struct Biol, 2009. **19**(6): p. 650-7.
217. Baer, C.E., et al., *Biochemical and spatial coincidence in the provisional Ser/Thr protein kinase interaction network of Mycobacterium tuberculosis.* J Biol Chem, 2014. **289**(30): p. 20422-33.
218. Rieck, B., et al., *PknG senses amino acid availability to control metabolism and virulence of Mycobacterium tuberculosis.* PLoS Pathog, 2017. **13**(5): p. e1006399.
219. Kaur, K., et al., *DevS/DosS sensor is bifunctional and its phosphatase activity precludes aerobic DevR/DosR regulon expression in Mycobacterium tuberculosis.* Febs j, 2016. **283**(15): p. 2949-62.
220. Kumari, P., et al., *Phosphatase-defective DevS sensor kinase mutants permit constitutive expression of DevR-regulated dormancy genes in Mycobacterium tuberculosis.* Biochem J, 2020. **477**(9): p. 1669-1682.
221. Labugger, R., et al., *Extensive troponin I and T modification detected in serum from patients with acute myocardial infarction.* Circulation, 2000. **102**(11): p. 1221-6.

222. Rammohan, J., et al., *CarD stabilizes mycobacterial open complexes via a two-tiered kinetic mechanism.* Nucleic Acids Res, 2015. **43**(6): p. 3272-85.
223. Kevorkian, Y.L., et al., *Rv0500A is a transcription factor that links Mycobacterium tuberculosis environmental response with division and impacts host colonization.* Mol Microbiol, 2022. **117**(5): p. 1048-1062.
224. Abramovitch, R.B., et al., *aprABC: a Mycobacterium tuberculosis complex-specific locus that modulates pH-driven adaptation to the macrophage phagosome.* Mol Microbiol, 2011. **80**(3): p. 678-94.
225. Chen, Y., B. Hagopian, and S. Tan, *Cholesterol metabolism and intrabacterial potassium homeostasis are intrinsically related in Mycobacterium tuberculosis.* PLOS Pathogens, 2025. **21**(5): p. e1013207.
226. Surya, W. and J. Torres, *Sedimentation equilibrium of a small oligomer-forming membrane protein: effect of histidine protonation on pentameric stability.* J Vis Exp, 2015(98): p. e52404.
227. Thomsen, M., *Determination of the Molecular Mass of Membrane Proteins Using Size-Exclusion Chromatography with Multiangle Laser Light Scattering (SEC-MALLS).* Methods Mol Biol, 2020. **2168**: p. 263-269.
228. Masson, G.R., M.L. Jenkins, and J.E. Burke, *An overview of hydrogen deuterium exchange mass spectrometry (HDX-MS) in drug discovery.* Expert Opin Drug Discov, 2017. **12**(10): p. 981-994.
229. Schuler, B. and H. Hofmann, *Single-molecule spectroscopy of protein folding dynamics--expanding scope and timescales.* Curr Opin Struct Biol, 2013. **23**(1): p. 36-47.
230. Zhang, M.S., et al., *Biosynthesis and genetic encoding of phosphothreonine through parallel selection and deep sequencing.* Nature Methods, 2017. **14**(7): p. 729-736.
231. Johnson, D.S., et al., *Genome-Wide Mapping of in Vivo Protein-DNA Interactions.* Science, 2007. **316**(5830): p. 1497-1502.
232. Sachs, K., et al., *Causal protein-signaling networks derived from multiparameter single-cell data.* Science, 2005. **308**(5721): p. 523-9.
233. Barford, D., A.K. Das, and M.P. Egloff, *The structure and mechanism of protein phosphatases: insights into catalysis and regulation.* Annu Rev Biophys Biomol Struct, 1998. **27**: p. 133-64.
234. Pullen, K.E., et al., *An alternate conformation and a third metal in PstP/Ppp, the M. tuberculosis PP2C-Family Ser/Thr protein phosphatase.* Structure, 2004. **12**(11): p. 1947-54.
235. Needham, E.J., et al., *Illuminating the dark phosphoproteome.* Science Signaling, 2019. **12**(565): p. eaau8645.
236. Wu, R., et al., *A large-scale method to measure absolute protein phosphorylation stoichiometries.* Nat Methods, 2011. **8**(8): p. 677-83.